INFORMATION TO USERS

The most advanced technology has been used to photograph and reproduce this manuscript from the microfilm master. UMI films the text directly from the original or copy submitted. Thus, some thesis and dissertation copies are in typewriter face, while others may be from any type of computer printer.

The quality of this reproduction is dependent upon the quality of the copy submitted. Broken or indistinct print, colored or poor quality illustrations and photographs, print bleedthrough, substandard margins, and improper alignment can adversely affect reproduction.

In the unlikely event that the author did not send UMI a complete manuscript and there are missing pages, these will be noted. Also, if unauthorized copyright material had to be removed, a note will indicate the deletion.

Oversize materials (e.g., maps, drawings, charts) are reproduced by sectioning the original, beginning at the upper left-hand corner and continuing from left to right in equal sections with small overlaps. Each original is also photographed in one exposure and is included in reduced form at the back of the book.

Photographs included in the original manuscript have been reproduced xerographically in this copy. Higher quality 6" x 9" black and white photographic prints are available for any photographs or illustrations appearing in this copy for an additional charge. Contact UMI directly to order.

UMI

University Microfilms International
A Bell & Howell Information Company
300 North Zeeb Road. Ann Arbor. MI 48106-1346 USA
313/761-4700 800/521-0600

Order Number 1341997

Effect of low vacuum on density and stress-strain-strength behavior of lunar soil simulant

Allen, Thomas Lyll, M.S.

The University of Arizona, 1990

U·M·I
300 N. Zeeb Rd.
Ann Arbor, MI 48106

EFFECT OF LOW VACUUM ON DENSITY AND STRESS-STRAIN-STRENGTH BEHAVIOR OF LUNAR SOIL SIMULANT

by

Thomas Lyll Allen

A Thesis Submitted to the Faculty of the

DEPARTMENT OF CIVIL ENGINEERING AND ENGINEERING MECHANICS

In Partial Fulfillment of the Requirements
For the Degree of

MASTER OF SCIENCE
WITH A MAJOR IN CIVIL ENGINEERING

In the Graduate College

THE UNIVERSITY OF ARIZONA

1 9 9 0

STATEMENT BY AUTHOR

This thesis has been submitted in partial fulfillment of requirements for an advanced degree at The University of Arizona and is deposited in the University Library to be made available to borrowers under rules of the Library.

Brief quotations from this thesis are allowable without special permission, provided that accurate acknowledgement of source is made. Requests for permission for extended quotation from or reproduction of this manuscript in whole or in part may be granted by the head of the major department or the Dean of the Graduate College when in his or her judgement the proposed use of the material is in the interests of scholarship. In all other instances, however, permission must be obtained from the author.

SIGNED: 

APPROVAL BY THESIS DIRECTORS

This thesis has been approved on the date shown below:

 8-27-90

C. S. Desai — Date
Professor of Civil Engineering
and Engineering Mechanics

 8-28-90

H. Saadatmanesh — Date
Assistant Professor of Civil Engineering
and Engineering Mechanics

ACKNOWLEDGEMENTS

The author would like to thank Clara Thompson for her support during the writing of this manuscript and Mr. Bill Green, P.E., Soils Consultants, Inc. for the motivation to attempt graduate studies.

The basic concept of the research and design of the test devices herein were developed by Dr. C. S. Desai. The modified design and construction of the devices were accomplished with participation of Dr. C. S. Desai, Dr. H. Saadatmanesh, and the author; the devices were fabricated with the assistance of the staff in the Mechanical Shop, Department of Civil Engineering and Engineering Mechanics, University of Arizona; Tucson, Arizona.

This research was funded in part by Grant No. 347184 from the NASA Space Engineering Research Center, University of Arizona; Tucson, Arizona.

TABLE OF CONTENTS

page

TABLE OF CONTENTS (Continued)

LIST OF FIGURES

page

LIST OF FIGURES (Continued)

LIST OF TABLES

ABSTRACT

Proposals to establish a manned base on the moon have necessitated the in-depth study of the engineering properties of the lunar regolith. In this investigation, the density and stress-strain-strength behavior of a lunar soil simulant in low vacuum were studied. A lunar soil simulant was produced from crushed terrestrial basalt rock and a vacuum triaxial stress device was designed, fabricated, and operated. The simulant was compacted to ultimate density, subjected to one-dimensional stress while constrained, and then subjected to triaxial states of stress. Vacuum levels ranged from 760 torr to 0.004 torr. Confining stresses considered were 0.10 MPa, 0.14 MPa, and 0.17 MPa. Low vacuum was found not to have any significant effect on the density or the stress-strain-strength behavior of the simulant as compared to results of tests at atmospheric pressure.

CHAPTER 1 INTRODUCTION

Mankind has been active in outer space continuously over the past three decades. The early space programs proved that man had the capability to orbit the earth and could survive in outer space for limited time periods. Recent advances in space technology, including the Soviet Soyuz and the U.S. Skylab missions, demonstrated that man can live and work in space for very long periods of time. The research conducted on these missions; related to manufacturing, astronomy, remote sensing, and communications, indicated that construction of a permanent orbitting station or lunar base would be beneficial. A major obstacle in the construction of a large facility in space is the cost of placing terrestrial materials in orbit. This is the motivation behind the study of extraterrestrial construction materials.

As a source of raw material for construction in space the obvious choice is our nearest neighbor, the moon. The most immediate uses for lunar material would be as radiation shielding for a lunar base or orbitting work station and to provide support and traction for lunar vehicles, Land (1985). A shift from purely analytical studies of the lunar

regolith to the utilization of lunar soil as a construction material requires research into methods of consolidating the dry, granular soils to form suitable structural components. It is the strength characteristics of dry, compacted lunar soil that is the focus of this research.

Until the U.S. Surveyor program and the Soviet Union's LUNA program, surface properties of the moon could only be assessed by earth-based optical, thermal, radio, and radar observations. These methods of analysis could not suitably predict lunar surface properties to insure that the lunar surface could support the landing of a spacecraft and human activity. The Surveyor program provided the first data concerning mechanical properties of lunar soil . Results of the simple tests performed by the robot arm of Surveyors III and VII guided engineers in the design of the Apollo landing modules and lunar roving vehicles, Scott (1969).

The astronauts of the Apollo program took the next step by conducting well planned soils investigations on the lunar surface and retrieving soil and rock samples for study on earth. It is the results of these studies that provide first hand knowledge of the lunar regolith. The completion of the Apollo program ended a significant exploratory phase of mankind's utilization of outer space; and although the terrestrial study of lunar soil samples continues to date, this ongoing research is primarily aimed

at analysis rather than development of resources on the moon.

Meaningful experiments in the densification of lunar soils would require a large amount of lunar material. In addition, for results of such research to have applications in the 10^{-24} torr vacuum of space or the 10^{-14} torr vacuum found on the lunar surface, the process must take place in a vacuum. Supplies of returned lunar soils are very limited, and the quantities required for a large scale study of the properties of the lunar regolith are unavailable. No exact lunar soil simulant; one that has all the chemical, mechanical, and environmentally induced properties of actual lunar soil; exists on earth. However, a substitute for lunar soil may be prepared from various terrestrial materials to simulate some aspects of actual lunar soil pertinent to a particular study. The funding and logistics necessary to perform experiments on lunar soils or simulants in the perfect vacuum of space make that approach impractical. For these reasons, investigations of the compaction and strength characteristics of dry granular lunar soils need to be conducted using simulants in a laboratory vacuum chamber.

The objectives of this investigation were to illustrate the effects of cyclic loading on density under low vacuum conditions and to observe the stress-strain-strength

properties of lunar soil simulant in low vacuum. Essential to achieving these objectives were the production of a lunar soil simulant from terrestrial igneous rocks; and the design, fabrication and successful operation of a vacuum chamber in which the simulant could be subjected to a triaxial state of stress.

CHAPTER 2 LITERATURE REVIEW

2.1 Porosity of Lunar Soil Simulant in Vacuum

Early researchers, Vey and Nelson, (1965) determined the porosity attained by lunar soil simulants when deposited under various vacuum levels. Three different soil samples were used: silica flour with 90% of particles having diameters between 2 and 26 microns; ground olivine with 90% of particles having diameters between 2 and 60 microns; and ground olivine with 90% of particles having diameters between 0.7 and 15 microns.

The materials were first placed on a No. 10 sieve. Arching of the soil across the sieve openings prevented the soil from falling through as long as the sieve remained stationary. When the pressure in the test chamber had been reduced to that at which the experiment was to be performed, the shaft holding the sieve was vibrated by hand through a steel bellows attached to the top of the vacuum chamber and the soil fell freely into small containers below. The chamber was then vented to the atmosphere slowly; the containers were removed, levelled and weighed and the porosity computed. Experiments were performed at absolute pressures ranging from atmospheric (760 torr) to

4.4×10^{-9} torr.

Results showed that porosities attained by soils deposited under low vacuums (10^{-3} torr) were less than those attained in atmosphere. However, at higher vacuum levels the porosity increased with an increase in vacuum, and in the case of silica flour, for vacuums of 10^{-7} torr or higher it was greater than when deposited in atmosphere.

The increase in porosity in both soils was attributed to the development of interparticle forces. These forces may be either attractive or repulsive depending on the mineralogical composition of the soil and the vacuum level.

2.2 Unconfined Compressive Strength of Prestressed Lunar Soil Simulant

Nowatzki (1971) conducted a study to show that loading history and the environmental influence of heat and ultrahigh vacuum affect the unconfined compressive strength of a heterogeneous mass of granular material. An increase in bulk compressive strength was interpreted to be a manifestation on a macro scale of an increase in the amount and / or type of bonding between particles.

Two materials were investigated: basalt from Somerset, New Jersey, and ilmenite from St. Urbain, Quebec, Canada. Samples of each of the rock materials were crushed and ground in a ball mill to obtain a range of particle sizes

from which a mixture would be made having a grain size distribution similar to that reported at the Apollo 11 site. The specific gravity of each of the materials was determined with a pyncnometer and reported as 2.99 for the basalt and 4.62 for the ilmenite.

A known weight of each sample was placed in a stainless steel split-mold cylinder with an inside diameter of 1.905 cm (0.75 in.), an outside diameter of 3.175 cm (1.25 in.), and approximately 5.08 cm (2.00 in.) high. Four such samples were placed in a special loading frame and the same compressive prestress was applied to each cylinder. Three prestress values were used: 0.156 kb (15.6 MPa), 0.468 kb (46.8 MPa), and 0.780 kb (78.0 MPa). After the predetermined prestress was applied, the load was maintained on the samples by a specially designed piston locking device. In this way one-dimensional loading with lateral constraint was obtained. Without releasing the load, the assembly was placed in a vacuum chamber and heated and pumped down to the 10^{-11} torr range. For each set of samples prepared in the quadruple mold, a single control sample was prepared in another mold that was not subjected to vacuum but instead was placed in an oven at 100 ° C for the duration of the pumpdown and vacuum exposure of the other four samples.

After being exposed to vacuum for at least 24 hrs., the

samples were removed from the molds. The samples exposed to heat and vacuum resembled cylindrical bricks which could stand intact without lateral support. An INSTRON testing instrument Model TM-M was used to load the sample axially at a rate of 0.1 cm (0.04 in.) per minute. The load-deformation curve was obtained directly on a strip chart recorder. The porosity of the samples was computed after loading.

Results showed that the vacuum samples possessed a higher induced strength than the samples not subjected to vacuum at all porosities (prestress levels). This increase in strength was significant and was from 200% to 300% for basalt at high prestress levels. The percent gain in strength was different for the two materials.

These results indicated that (a) Prestress alone causes samples of granular material to acquire an increase in compressive strength, (b) exposure of prestressed samples to baking and ultrahigh vacuum resulted in additional increases in compressive strength; heating seemed to be the predominant factor in the strength gain process, and (c) the mineralogical composition of the aggregate particles influences the amount of strength increase.

The increase in strength was attributed to an increase in surface bonding forces that resulted from a complex interaction of thermal and mechanical stresses. The test

conditions had some similarity to environmental conditions on the moon which could have altered some of the bulk properties of lunar soil and rock.

2.3 Compressibilty and Direct Shear Tests on Granular Materials in Vacuum

In addition to measurements of porosity in vacuum discussed above, Vey and Nelson (1965) conducted direct shear tests in their investigation to determine the effect of vacuum on shear strength parameters. Direct shear tests were used to overcome the limitations on attainable vacuum levels imposed by the outgassing of membranes required in triaxial tests.

Experiments were conducted using the silica flour and the finer grain sized olivine. The porosity of the soil samples used in the tests was controlled by placing the soil in the apparatus at the highest porosity achievable and then consolidating it under the maximum normal stress used in the test. The average shear stress required to produce movement of the upper ring of the shear box was plotted as a function of the normal stress to determine the Mohr's rupture diagram in the conventional manner. Pressure levels ranged from 760 torr to 8×10^{-10} torr.

For soil samples prepared in the atmosphere and then placed in the vacuum chamber, it was observed that the

vacuum in the soil pores was considerably less than that recorded in the chamber. Direct shear tests showed that apparent cohesion and the internal friction of the silica flour increased under vacuum. The internal friction of olivine also increased under vacuum but its apparent cohesion appeared to decrease.

As with the increase in porosity for both soils, the effects on the apparent cohesion were attributed tc the development of interparticle forces. These forces may be either attractive or repulsive depending on the mineralogical composition of the soil and the vacuum level. The authors concluded that the level of particle cleanliness; that is, the amount of adsorbed gasses present on particle surfaces; has an important influence on stress-strain behavior.

In order to explore the adhesion and compressibilty characteristics of lunar soil simulant, Johnson, et. al. (1970) performed experiments at various vacuum levels from atmospheric down to ultra-high vacuum. The granular medium used was comminuted basalt rock from near Madras, Oregon; all of which passed the No. 250 U.S. Standard Sieve.

The rock powder was placed in a 2.54 cm (1 in.) diameter metal ring of 1.78 cm (0.7 in.) depth. To facilitate outgassing, narrow vertical slits were cut in the sides of the ring. A loading plate 2.03 cm (0.8 in.) in diameter was

placed on top of the powder in the ring and an axial load was applied. The powder had an initial void ratio of 1.75 and as the loading plate moved downward at 0.013 cm/min. (0.005 in./min.) measurements were made of the void ratio, e, and the applied pressure, p. The results were presented as a plot of e vs. p for pressures of 740 torr, 10^{-8} torr, and 10^{-10} torr.

To avoid vibrating the sample, sorption pumps were used for rough pumping and a sublimation pump and an ion pump were used to achieve vacuums in the range of 10^{-10} torr. The 10^{-8} torr tests were performed without prior bakeout but the 10^{-10} torr tests involved a system bakeout at 200° C for 18 hrs. and a superimposed bakeout of the soil sample by a small adjacent heating coil at 300° C for 3 hours. The exposure to high temperature was intended to increase the surface cleanliness of the soil grains.

The results of the in-air and in-vacuum tests demonstrate that the compressibilty of the basalt powder is less for samples exposed to bakeout and pumpdown to 10^{-10} torr than for similar samples tested at atmospheric pressure. Due to a leak that developed during one test that was scheduled to be conducted at 10^{-10} torr, the sample achieved only 10^{-8} torr after bakeout. The results of this test were very similar to the 10^{-10} torr test results and not at all like other 10^{-8} torr test results. This observation lead to the

conclusion that vacuum level does not necessarily determine the degree of particle surface cleanliness and that more research was needed to define the effects of vacuum and heat on the compressibilty of granular soils.

Carrier, et. al. (1973) performed tests in which the compressibility of returned lunar soil was compared with that of a terrestrial simulant. They tested a 200g sample of lunar soil taken near the Apollo 12 Lunar Module landing site. The sample had previously been stored for over a year at 10^{-9} torr and had experienced a pressure of only 10^{-2} torr prior to storage. It was assumed that very little atmospheric contamination of the sample had taken place.

Two oedometer and three direct shear tests were performed on the sample under vacuum. The samples were prepared at the Lunar Research Laboratory in the F-401 glove test chamber at a pressure less than 2×10^{-6} torr. Prepared samples were placed in an ultra-high vacuum (UHV) chamber within the F-401. Attached to the UHV chamber were stainless steel bellows to transmit normal and shear forces to the samples. The UHV chamber was removed from the F-401 and evacuated to the 10^{-8} torr range. Shear and normal forces were measured by load cells and displacements were measured by LVDTs mounted parallel to each bellows.

The first sample was placed at $1.84 g/cm^3$, compressed in four increments to 31.21 kN/m^2 and sheared (Test 1). A

normal load of 1.93 kN/m^2 was left on the sample as the shear box was moved back into position. The sample was then recompressed in four increments to a normal stress of 69.92 kN/m^2 and resheared (Test 1b).

For the second test, the sample was placed in the shear box in as loose a state as could be attained (1.67g/cm^3). It was compressed in a series of four increments, including rebound and compression stages, to a final stress of 67.51 kN/m^2 and sheared.

For comparison, two oedometer tests were performed in air on basalt sand simulant. The simulant had a grain size distribution similar to the lunar soil and was placed at the same initial void ratio.

At the lower density, the lunar soil had a higher compressibilty than the simulant. The lunar soil skeleton did not rebound to any significant extent. The typical recompression index, C_R, was 0.003 and the typical virgin compression index, C_C, was 0.06. Compression during each increment was virtually instantaneous.

The lunar soil had a shear strength of only 65% of the simulant shear strength and reached failure at a shear strain of about 4%. The change in the height of the sample in all tests was ranged from 1% to 3%. Cohesion was estimated in the range of 0 kN/m^2 to 7 kN/m^2, and the angle of internal friction was estimated to be 28 degrees for the

loose sample and 34 degrees to 35 degrees for the medium dense samples.

Gas pressure measurements were made with a residual gas analyzer during the tests. Pressure bursts occurred during compression and shear when the previous maximum stress had been exceeded. These pressure bursts could not be attributed to terrestrial contamination.

Conclusions were that lunar soil is significantly different from ground basalt simulants. The higher compressibility and lower shear strength of the lunar soils was attributed to particle crushing within the sample. Due to grain crushing, lunar soil samples cannot be retested indefinitely. The observed gas bursts may provide a means of measuring the past maximum stress for an undisturbed lunar soil sample.

2.4 Triaxial and Cohesion Tests of Lunar Soil Simulant in Atmosphere and Low Vacuum

The U.S. Army Engineer Waterways Experiment Station evaluated strength characteristics of a lunar soil simulant to predict the performance of the wheels of the U.S. Lunar Roving Vehicle, Melzer (1974). Of primary interest were angle of internal friction, cohesion, and cone penetration resistance. The three test methods for evaluating these parameters were vacuum triaxial test, trenching in a soil

bin and a standard mechanical cone penetrometer.

The soil was prepared by grinding basaltic rocks into very small particles. These were then selectively screened and combined to form a soil with a grain size distribution approximating that of the lunar soil samples collected during the Apollo 11 and 12 missions. The soil and simulant were well graded with sizes ranging from 5 mm to less than 0.001 mm.

The angle of internal friction of the simulant was evaluated as a function of relative density and absolute density by conducting triaxial tests on oven dried material. Samples were 7 cm in diameter and 15 cm high. Confining pressures were constant during each test and were applied by creating a vacuum in the sample which was surrounded by a rubber membrane. This pressure was measured by a simple differential mercury manometer. The axial load was applied at a constant strain rate of 0.2 mm/min until 15% axial strain was reached. Volume change was estimated by measuring the specimen circumference at different times during the test. Due to the elastic properties of the rubber membrane, the measured deviator stress had to be corrected by the method described by Bishop and Henkel (1962).

Three series of vacuum triaxial tests were conducted at confining pressures of 3.5, 6.9 and 20.7 kpa. For the first

two series, the sample densities were 1.55, 1.65 and 1.84 g/cm^3. For the series at 20.7 kpa the densities were 1.58, 1.65 and 1.84 g/cm^3.

The results show that at a given density, the angle of internal friction decreases with increased confining pressure. The rate of decrease of friction angle increased with increasing relative density.

The cohesion of the soil simulant was measured by a trenching test. The soil simulant was prepared in a soil bin to the desired density. The tests were conducted at atmospheric pressure with soil moisture contents at 0.9% and 1.8%. A trench was then dug in the bin 1 cm at a time until the sides of the trench failed. Due to the shallowness of the bin, 35 cm, a surface load was required to fail the wall. The cohesion was evaluated by the Coulomb wedge method and by slope stability analysis. The results of these two methods were averaged. In general, the results showed that apparent cohesion increased with relative density at a given moisture content; and for a given relative density or density apparent cohesion increased with increased moisture content.

The cone penetration tests were conducted in a soil bin 1 m wide and 35 cm deep. A WES standard cone penetrated the sample at various points in the bin at a constant rate of 0.03 m/s. The cone resistance was measured throughout the

full depth of penetration by a load cell mounted at the top of the penetrometer shaft.

Two series of penetration tests were conducted, one at the moisture content of 0.8%, and the other at 1.8%. The dry densities ranged from 1.47 to 1.89 g/cm^3. The results show that moisture content influences penetration resistance at a given density only if the density is less than 1.80 g/cm^3.

CHAPTER 3 SCOPE OF RESEARCH

3.1 Production of Lunar Soil Simulant

For the investigation of the strength properties of lunar soil compressed in a vacuum environment; a suitable simulant was produced by crushing a terrestrial igneous rock. By combining the resulting grains in proportions that match the lunar soil grain size distribution; 20 kg (44 lb) of lunar soil simulant were produced.

3.2 Pilot Compaction Study

An initial series of tests was performed using an existing vacuum chamber in which the lunar soil simulant was compacted by cyclic loading. Three different initial densities were considered. Vacuum levels ranged from atmospheric pressure to 4×10^{-3} torr. In the process, the author became familiar with the operation of the vacuum pumping system and the cyclic loading apparatus. The results of this study were useful for the design of new equipment and the specification of test procedures for subsequent work.

3.3 Vacuum Triaxial Stress Device

A vacuum chamber was designed and fabricated which was capable of containing a controlled vacuum for extended periods of time. The device allowed input of compactive effort to a simulant sample while under vacuum, and provided a means of subjecting the compacted sample to triaxial states of stress.

3.4 Density/Vacuum/Cyclic Loads Tests

Samples of lunar soil simulant were compacted by cyclic loading from the same initial density and at various vacuum levels until an ultimate density was achieved. Measurements of density, cycles of loading, and vacuum levels were recorded. The results were analyzed to determine the relationships between these three variables.

3.5 Constrained Compression Tests

The compacted samples were loaded then unloaded vertically while constrained laterally, and axial stresses and strains were recorded. The data were analyzed to determine the compression and re-compression indices of the simulant at different levels of vacuum.

3.6 Vacuum Triaxial Tests

Lunar soil simulant specimens which had been compacted at various vacuum levels, and had undergone the above tests were subjected to states of triaxial stress while in vacuum. The axial stress on the samples was increased while the confining stress was held constant. Measurements of axial stress and strain were analyzed to determine stress-strain-strength characteristics at different levels of vacuum.

CHAPTER 4 THE LUNAR SOIL SIMULANT

4.1 Properties of the Lunar Soil Simulant

The properties of a soil simulant should match as closely as possible those of the soil being modelled. However, lunar soil has some characteristics which are difficult to reproduce from terrestrial materials. Constant bombardment of exposed lunar soils by cosmic radiation has altered the surfaces of the particles which make up the lunar regolith. Energy released by meteor impacts or volcanic activity has melted some particles to form minute glassy spheroids. Other particles consist of agglutinates of fine sands which may have been sintered by high heat, Carrier, et. al. (1973). Although some lunar soil simulants are available which contain adequate duplicates of these components of the lunar regolith; for the purposes of this study, producing a simulant matching the grain size distribution of lunar soil was considered of primary importance.

The simulant used in this study was crushed basalt rock from the Pomona Flow near Hanford, Washington. The specific gravity of the particles was found to be 2.86 as determined by the author according to the American Society of Testing and Materials specification ASTM-D 854. Returned lunar

soils were found to have a specific gravity of 3.1, Costes, et. al. (1970). A grain size distribution curve for the simulant is shown in Figure 4.1 along with the particle size distribution of the bulk of the soil returned from the moon, Carrier and Mitchell (1989). The maximum particle size of simulant used in this investigation was 0.600 mm. This was an arbitrary cut off point and larger particles may be added for future studies.

A hydrometer analysis (ASTM-D 422-80) was conducted on the material which passed the No. 200 standard sieve to define the distribution of the smaller grain sizes. The chemical composition of the simulant and that of some returned lunar soils are presented in Table 1, Fuenkajorn and Daemen (1986), Taylor (1975). Although the composition of the simulant did not exactly match that of lunar soil, the differences were deemed not significant for the purpose of this investigation.

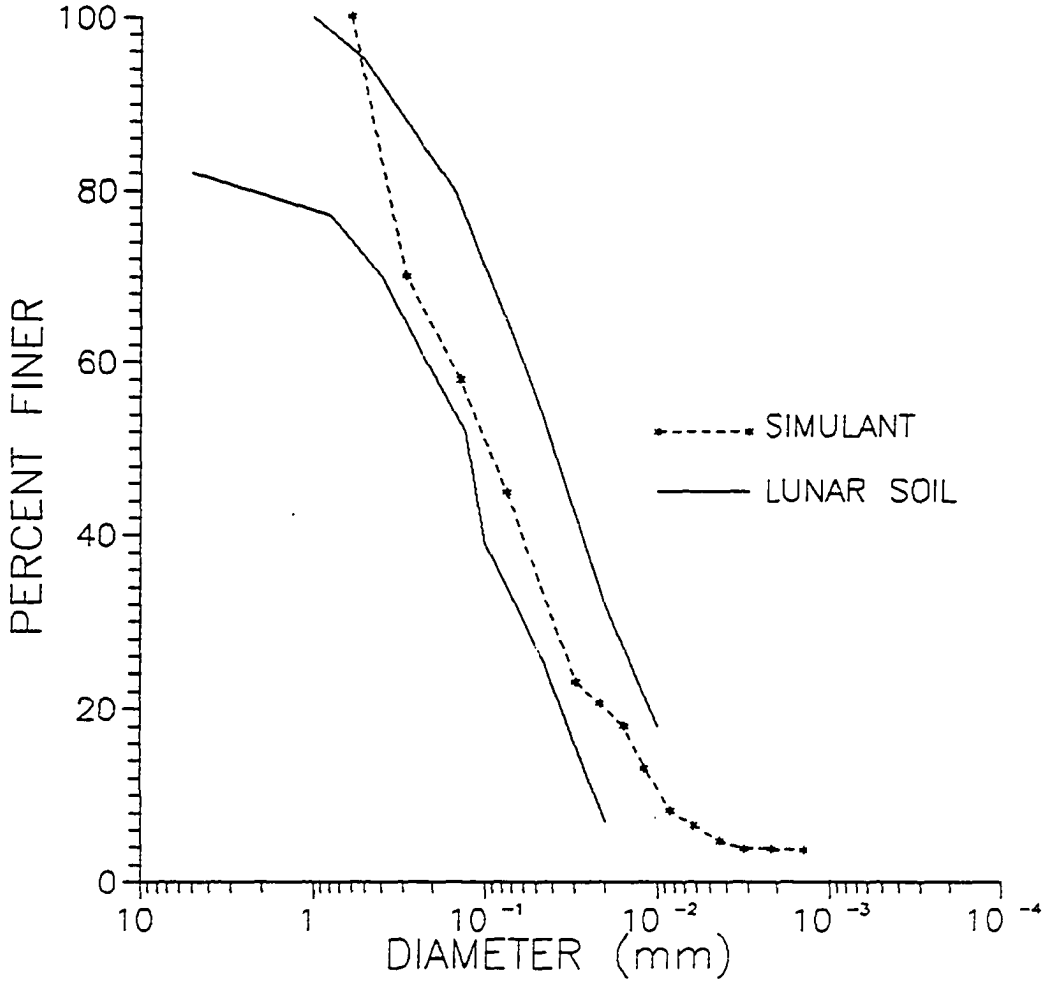

Fig. 4.1. Grain Size Distribution of Actual and Simulated Lunar Soil

Table 1

Chemical Composition (% by weight)

	Simulant	Lunar Soils **	
Compound	Pomona Basalt *	Maria	Highlands
SiO_2	48.0 - 50.0	45.4	45.5
Al_2O_3	13.5 - 16.0	14.9	24.0
TiO_2	1.6 - 3.2	3.9	0.6
FeO	7.0 - 12.5	14.1	5.9
MnO	0.20 - 0.25	--	--
MgO	4.3 - 6.5	9.2	7.5
CaO	8.3 - 10.3	11.8	15.9
Na_2O	2.7 - 3.0	0.6	0.6
K_2O	0.5 - 1.5	--	--
Fe_2O_3	1.9 - 4.6	--	--

*(Fuenkajorn and Daemen, 1986)

**(Taylor, 1975)

4.2 Lunar Soil Simulant Production

The basalt rock gravel was initially crushed in a roller-crusher until all particles passed the 2 mm sieve. This coarse sand was placed in a ceramic ball mill and ground for several days until it was reduced to rock powder. The sample was then shaken through a stack of U.S. Standard sieves to separate the various size constituents. By recombining the different sized particles in the correct proportions, 20 kilograms of satisfactory lunar soil simulant were produced.

CHAPTER 5 PILOT STUDY

5.1 Vacuum Compaction Chamber

The vacuum compaction chamber consisted of a hollow aluminum cylinder with a teflon liner, a loading piston, vertical actuator shaft, and ports to provide and measure vacuum. Figure 5.1 shows a cut-away drawing of the chamber. The total length was 38 cm (15 in.) and the top and bottom flange diameters were 24.9 cm (8 in.). The inside diameter of the teflon liner was 7.62 cm (3.0 in.) with the loading piston having a slightly smaller diameter of 7.49 cm (2.95 in.). This allowed application of vacuum from both the top and bottom of the sample. The chamber was sealed at the top and bottom flanges by single rubber "O-rings" compressed by tightening eight bolts in a circular pattern.

The 2.54 cm (1.00 in.) diameter actuator shaft rode in a brass "Oil-Lite" bushing and required an application of high vacuum silicon grease to seal satisfactorily. The upper and lower ports were connected to a common line from the vacuum system by 1.905 cm (0.75 in.) outside diameter brass tubing. To allow for easy disassembly of the chamber, a small section of the connecting tubing was replaced with

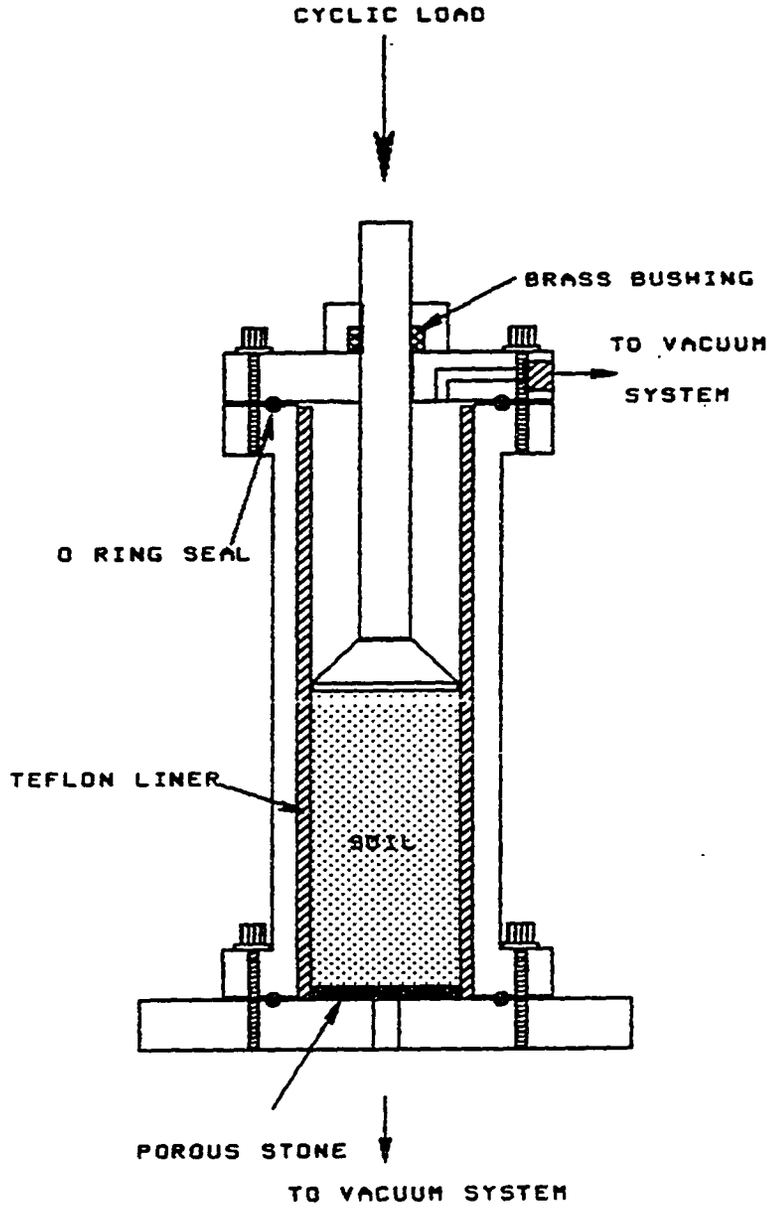

Fig. 5.1. Vacuum Compaction Chamber

rubber vacuum hose. A gate valve was placed between the common junction and the pumping system to provide a control of the pressure in the chamber.

5.2 Vacuum Pumping System

The vacuum pumping system consisted of A Seargent-Welch mechanical fore pump and a CVC oil diffusion pump capable of providing an ultimate vacuum pressure of less than 10^{-4} torr. These were used to pump down the chamber and simulant to a pressure of about 4×10^{-3} torr. No heating of the chamber was necessary for this low vacuum and the system design did not allow for the application of high temperatures. A small turbine fan was required to force air past the cooling fins of the diffusion pump to prevent the pump from overheating. To increase the efficiency of the vacuum pumps, a liquid nitrogen-cooled vapor trap was connected in the vacuum line between the pumps and the gate valve. Pressure in the chamber was measured by a digital Pirani vacuum gauge and two vacuum sensors; one at the top and one at the bottom of the chamber. Figure 5.2 shows a schematic diagram of the pumping system and compaction chamber.

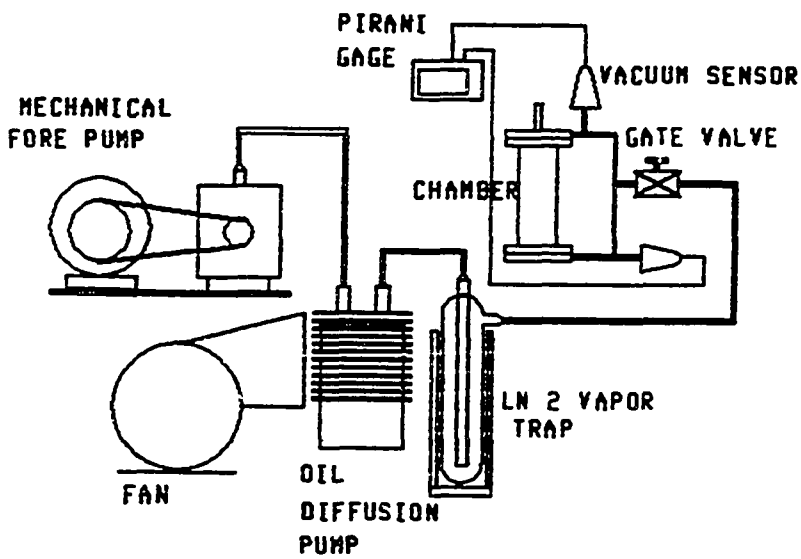

Fig. 5.2. Vacuum Pumping System and Test Chamber

5.3 Cyclic Loading System

Cyclic loading was provided by an MTS hydraulic system and loading frame. The sinusoidal loading pattern was controlled by an MTS Model 436 controller and function generator. Digital readouts of load and sample deformation were provided by a 44.5 kN (10 kip) load cell and an LVDT through an MTS Model 406 controller and a Tectronix digital voltmeter. The LVDT was calibrated by comparing voltage readouts with readings from a dial gage accurate to 0.001 inch (0.003 cm). Regression analysis revealed that a change in voltage could be converted to centimeters by multiplication by 1.3238 cm/volt.

5.4 Test Procedures

All lunar soil simulant samples had an initial height of 15.24 cm (6.00 in.) and a diameter of 7.62 cm (3.00 in.). Three different initial densities were considered; therefore, because the volume of each sample was the same 695 cm^3 (42.4 in^3), three different weights of simulant were used.

The lowest initial density, ρ_1, was determined by sifting the simulant into the chamber until it reached a height of 15.24 cm (6.0 in.) The weight of soil required was 1.075 kg which was divided by the sample volume to give ρ_1 = 1.547

g/cm^3. The second density, ρ_2, was arbitrarily chosen to be 10% greater than ρ_1; thus a sample weight of 1.185 kg provided a density $\rho_2 = 1.705\ g/cm^3$. Similarly, ρ_3 was chosen to be 20% greater than ρ_1 and a sample weight of 1.290 kg resulted in $\rho_3 = 1.856\ g/cm^3$. Measurements of the in-situ density of actual lunar soil give values ranging from 0.75 g/cm^3 to 1.97 g/cm^3, Scott, et al (1971). Thus, the three simulant initial densities were representative of in-situ lunar soil densities.

Prior to testing, the soils were heated in an oven to at least 120 ° C for a period of not less than 24 hours. The correct weight of soil for a given density was placed in the chamber as loosely as possible; then, if necessary, it was tamped by hand with the piston assembly until a sample height of 15.24 cm (6.0 in.) was reached. Samples to be tested at atmospheric pressure were allowed to cool before being placed in the compression chamber. Samples tested in vacuum were immediately placed in the chamber upon removal from the oven and pumpdown was begun as soon as possible. Approximately 1.5 hours of pumping were required to reach a vacuum of 5×10^{-2} torr, and 24 hours were required for a vacuum of 5×10^{-3} torr. Cyclic loading was begun as soon as the desired vacuum was reached.

A mean load of 22.2 kN (5 kips) was applied to the specimen as required to induce a cyclic load varying from

8.9 kN (2 kips) to 35.6 kN (8 kips). This produced a cyclic stress on the 7.62 cm (3.0 in.) diameter sample varying from 1950 kPa (283 psi) to 7803 kPa (1132 psi). Figure 5.3 shows the cyclic loading pattern produced by the MTS 436 function generator. Cyclic loading commenced at a frequency of 1.1 cycles per second. Vertical deformation of the sample was recorded at zero load and at the mean load after 1, 10, 50, and 100 cycles, and every 100 cycles thereafter. Loading continued until changes in sample height of 0.003 cm (0.001 in.) or less per 100 cycles were observed. The density of the sample, derived from the changing specimen height, was plotted against the number of cycles of loading. These procedures were followed for each of the three initial densities at atmospheric pressure, 5×10^{-2} torr, and at 4×10^{-3} torr.

5.5 Results of the Pilot Study

The densities achieved by each of the samples for the three test pressures at selected numbers of cycles are presented in Table 2. The plots in Figures 5.4, 5.5, and 5.6 show the variation of specimen density with the number of load cycles for all test pressures with initial densities ρ_1, ρ_2, and ρ_3 respectively. Figures 5.7, 5.8 and 5.9 show the variation of density vs. load cycles for all initial densities at atmospheric pressure,

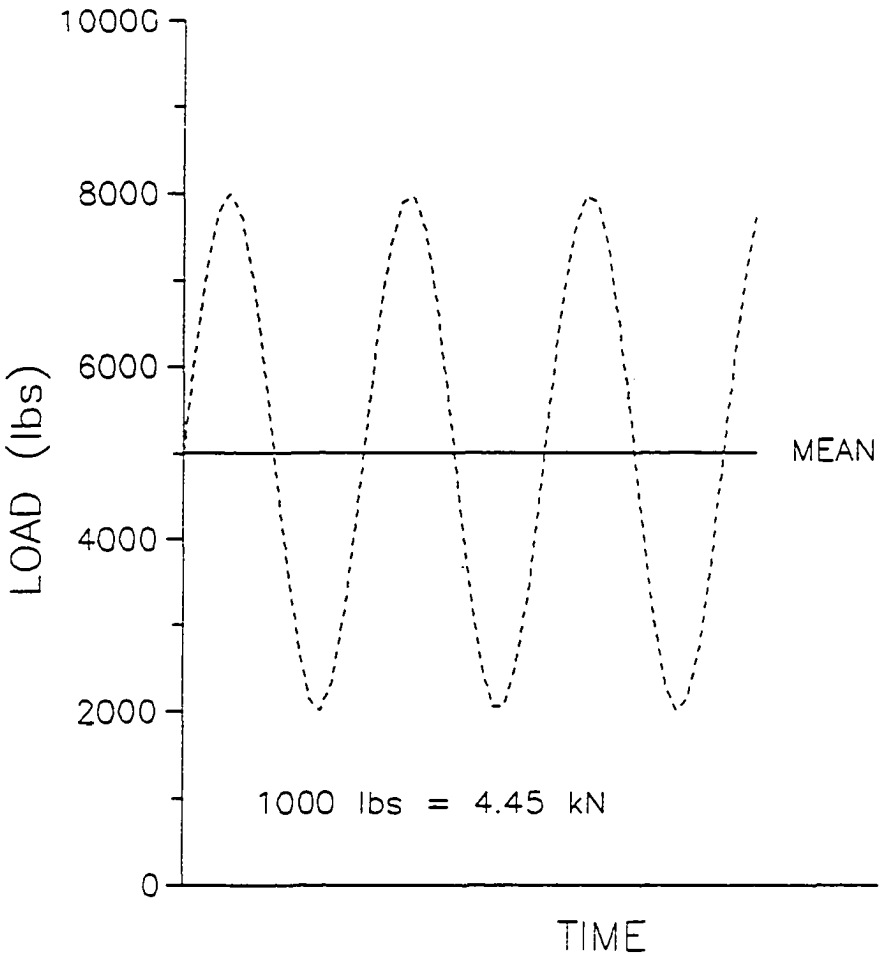

Fig. 5.3 Cyclic Loading Pattern

Table 2

Simulant Densities for Selected Numbers of Cycles of Loading : Pilot Study

Vacuum Level (torr)	Density (g/cm^3)					
	No. of Cycles					
	0	1	10	100	1000	4000
760	1.547	1.974	1.983	1.998	2.029	2.059
	1.705	1.956	1.966	1.979	2.006	2.029
	1.856	1.951	1.962	1.973	1.996	2.016
5×10^{-2}	1.547	1.947	1.955	1.967	1.993	2.020
	1.705	1.988	1.998	2.011	2.038	2.065
	1.856	1.993	2.003	2.017	2.044	2.070
4×10^{-3}	1.547	1.980	1.987	2.000	2.024	2.050
	1.705	1.985	1.990	2.003	2.027	2.049
	1.856	1.988	1.998	2.013	2.040	2.065

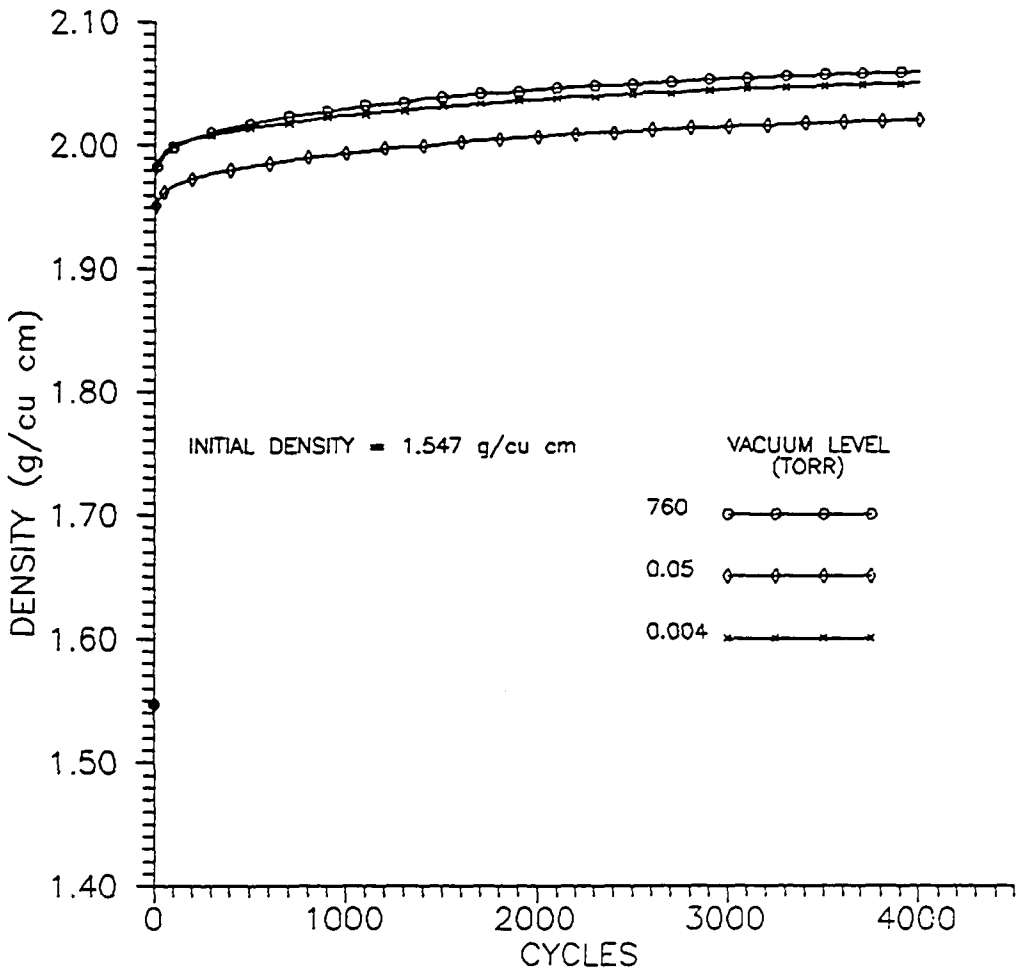

Fig. 5.4 Density vs. Number of Cycles

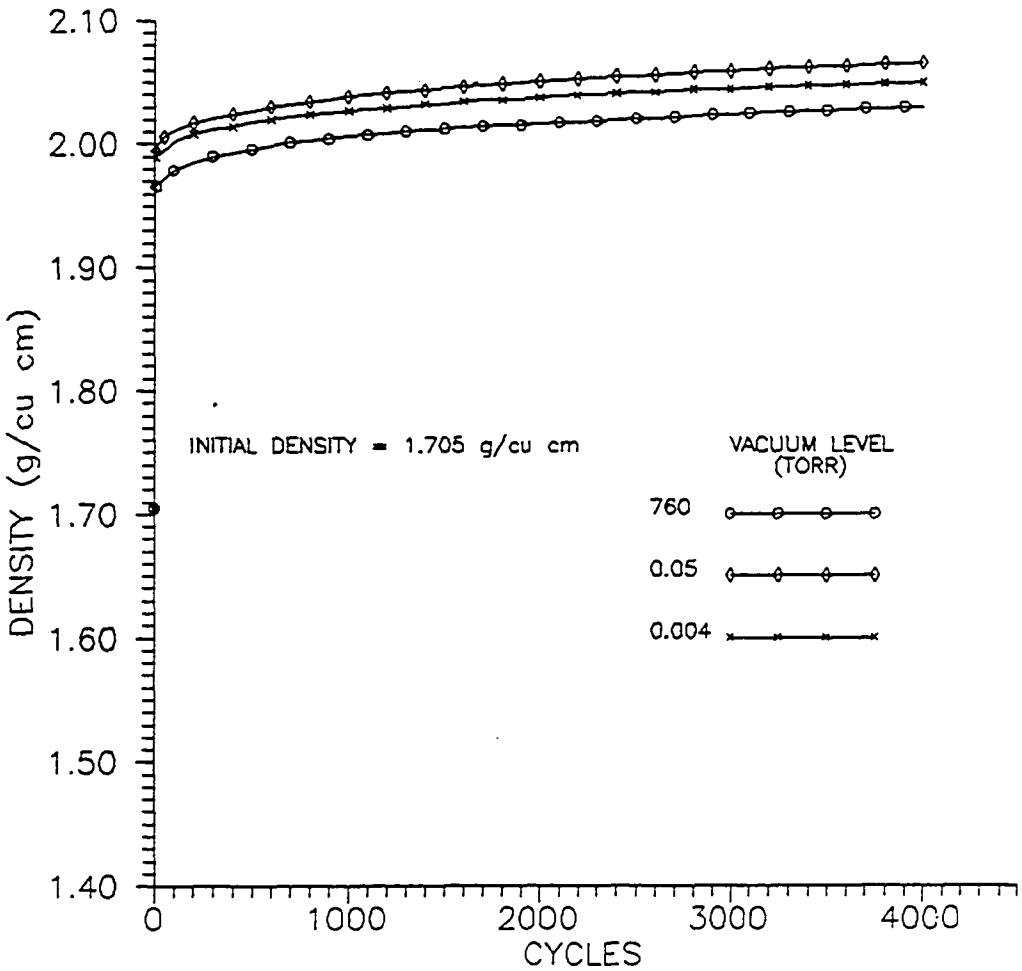

Fig. 5.5 Density vs. Number of Cycles

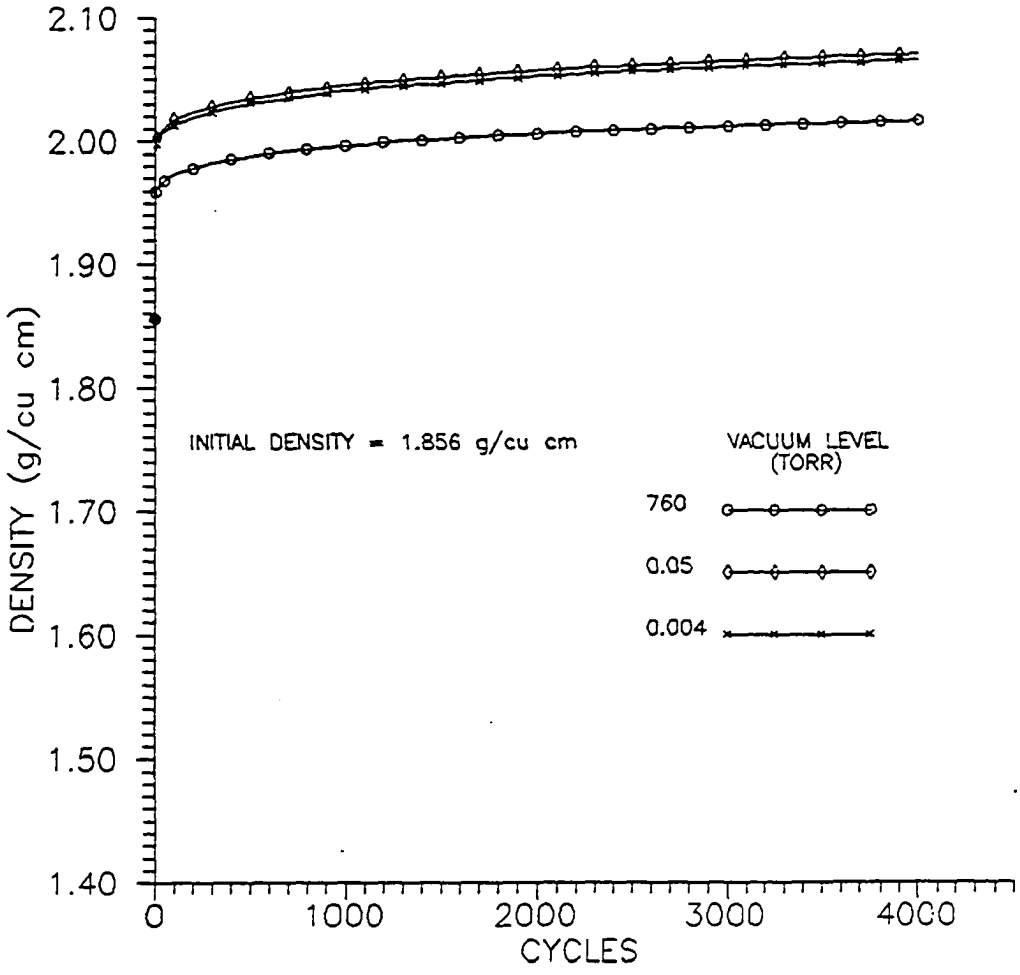

Fig. 5.6 Density vs. Number of Cycles

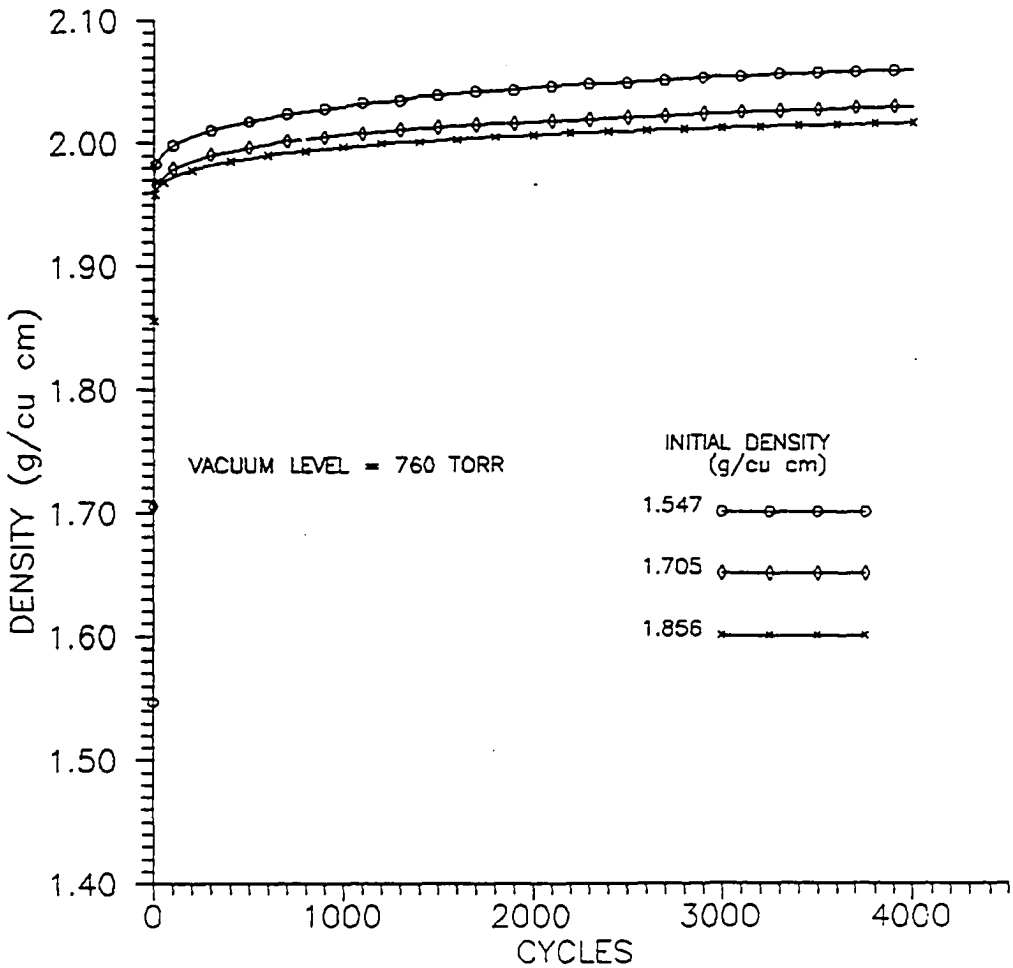

Fig. 5.7 Density vs. Number of Cycles

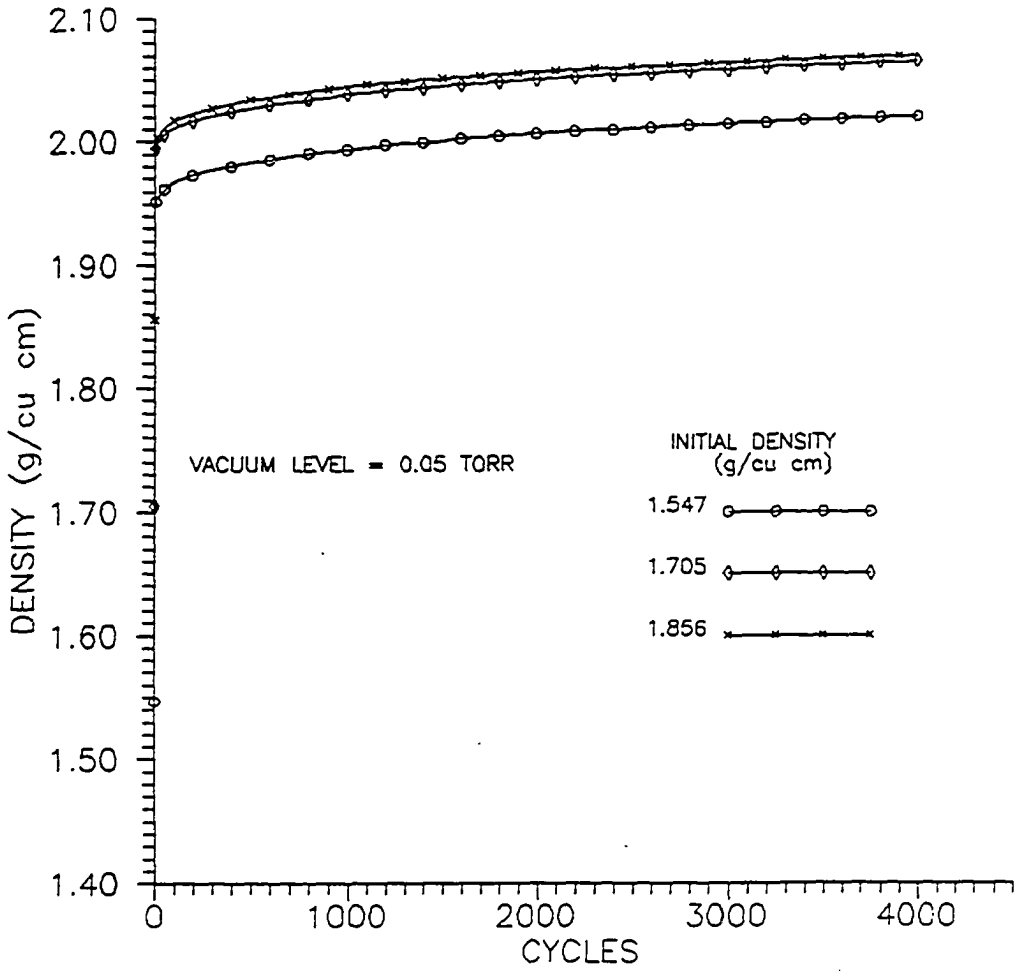

Fig. 5.8 Density vs. Number of Cycles

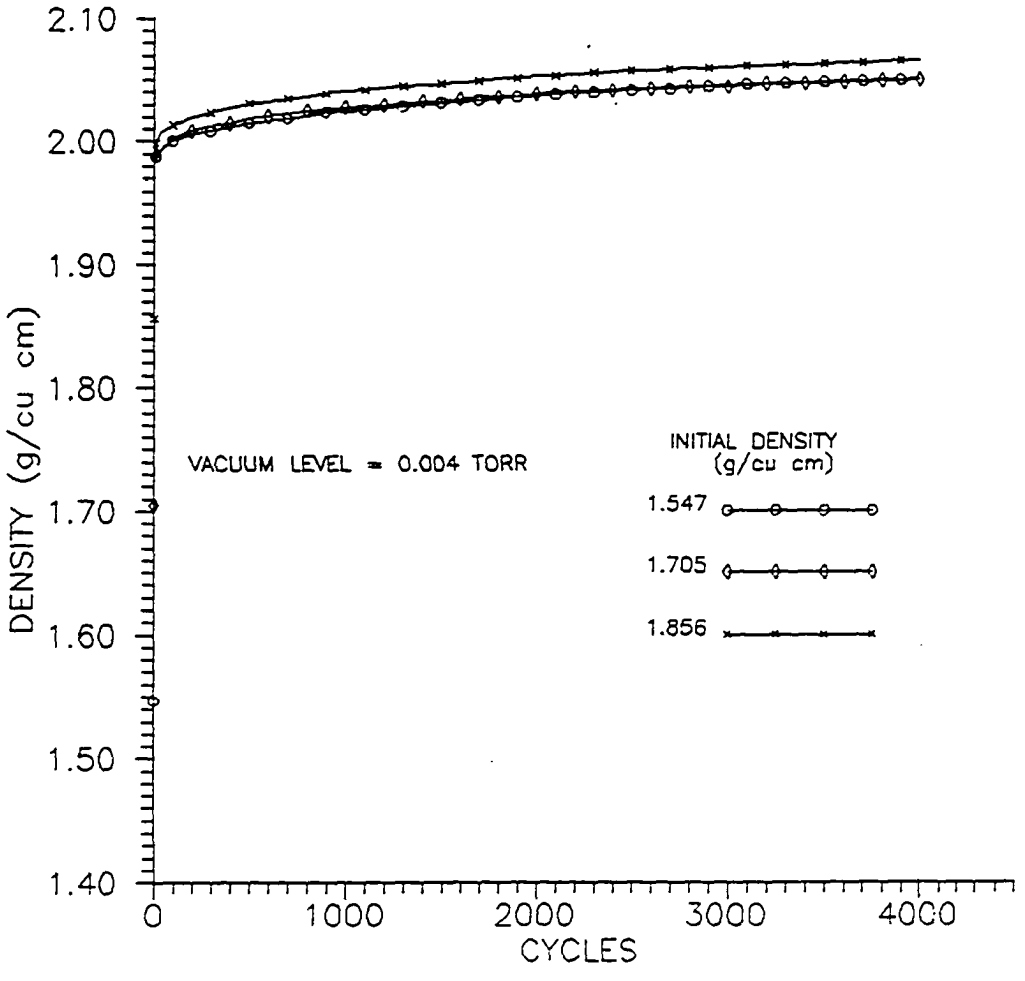

Fig. 5.9 Density vs. Number of Cycles

5×10^{-2} torr, and 4×10^{-3} torr, respectively. When the compacted specimens were inspected following the tests they were found to be very tightly consolidated. The consistency of the lunar soil simulant was that of very weathered concrete and significant effort with a chisel was required to remove it from the test chamber.

As shown in Figure 5.4, at atmospheric pressure the sample with the lowest initial density (1.547 g/cm^3) achieved the highest density after 4000 cycles of loading. The sample with the intermediate initial density (1.705 g/cm^3) had the intermediate final density; and the sample with the highest initial density (1.856 g/cm^3) had the lowest density after compaction.

At a vacuum of 5×10^{-2} torr (Figure 5.5) the order was reversed and the samples with the two highest initial densities reached almost the same density after compaction. The final density of the sample with the lowest initial density was significantly lower than the other two.

The final densities of all samples were very closely grouped at a vacuum of 4×10^{-3} torr (Figure 5.6). The sample with the highest initial density had a final density only slightly higher than that of the other two samples which had final densities that were virtually the same.

Figure 5.7 shows the densities that the samples that were

initially in the loosest state reached during compaction at the three vacuum levels. When compacted at atmospheric pressure and at 4×10^{-3} torr, the resulting final densities were very close and higher than the final density of the sample compacted at 5×10^{-2} torr.

Of the three samples with the intermediate initial density (Figure 5.8), the one compacted at a vacuum of 5×10^{-2} torr became the most dense after 4000 cycles of loading. A lower final density resulted when a similar sample was compacted at 4×10^{-3} torr; and when compacted at atmospheric pressure the lowest final density was observed for this initial density.

The behavior of the three soil samples compacted from the highest initial density, ρ_3, was similar to that of the samples compacted from the intermediate initial density, ρ_2. At 5×10^{-2} torr the highest final density was observed for the highest initial density and at atmospheric pressure the lowest final density resulted for this initial density. (Figure 5.9). A notable difference in this series of tests was that the final density of the sample compacted in atmosphere was significantly less than that of the samples compacted in vacuum.

5.6 Analysis and Conclusions

The results of the pilot study provided no clear definition of the compaction behavior of a lunar soil simulant in vacuum. Final densities resulting from these loading conditions were not significantly different. No definite trend was apparent when comparing compaction at different vacuum levels. It can be seen from Figures 5.4 through 5.9 that most of the compaction of the soil occurs during the first 100 cycles of loading. Also, all of the tests resulted in curves of similar shape. That is to say, that each sample exhibited the same change in density for a given change in the number of cycles of loading after about 100 cycles.

During the course of this pilot study, as the author became more familiar with the vacuum equipment on hand, several changes were made to the vacuum pumping system. The liquid nitrogen vapor trap was added, the original rubber tubing was replaced with an appropriate rubber vacuum line, and several small changes were made in the system configuration. The result at the end of the pilot study was the system shown in Figure 5.2. The apparatus is capable of pumping a well sealed chamber down to a pressure of less than 1×10^{-4} torr in 48 hours, 5×10^{-3} torr in 24 hours, and 5×10^{-2} torr in less than 1 hour. Thorough knowledge

of the characteristics of the vacuum pumping system was necessary before planning the test procedures for subsequent research.

Initial density may be eliminated as a variable in the investigation involving triaxial strength tests because it appears to have no significant influence on final density for the vacuum levels tested herein. Because most of the compaction of the sample occurred within the first 100 cycles of loading, in the future, sample density would be recorded more frequently during this interval. The magnitude of the compacting force for this pilot study was 35.6 kN (8000 lbs). If this load was reduced significantly a more accurate record of the compaction of the simulant may be obtained. As a first step in the triaxial study, for example, the compaction of the sample could be examined with a cyclic load of 6.7 kN (1500 lbs). If the number of cycles required to reach an ultimate density comparable to those achieved in this study was not excessive, the cyclic load would be reduced.

For this pilot study, the amount of time that the samples were exposed to vacuum was different for each vacuum level. Because the tests were run as soon as the pressure in the chamber reached the desired vacuum, isotropic pressure conditions had no opportunity to develop. To reduce the influence of this factor in future work the sample would be

held at the desired vacuum level for a specified time period.

CHAPTER 6 TRIAXIAL TESTS IN VACUUM

6.1 Vacuum Triaxial Chamber

For a meaningful simulation of the stress-strain-strength behavior of lunar soil, stress-strain tests need to be conducted under vacuum conditions. The lunar soil simulant should remain in vacuum continuously from the time it is placed in a chamber in a loose state, through the consolidation process, and until completion of all stress-strain tests.

The device developed for this investigation allows compaction of a soil specimen in vacuum under cyclic loading conditions, is capable of producing data to compute a precise constrained modulus of elasticity for the compacted soil, and allows for removal of the constraint and application of a controlled confining stress while the sample remains in vacuum. The conceptual design consisted of a rigid cylindrical sleeve inside a vacuum chamber within which a loose sample could be compacted. A mechanism outside the chamber would provide a lifting force to remove the sleeve from around the sample after compaction. As the sleeve was raised, a flexible barrier would surround the sample. A fluid pressure would provide a radial confining stress on the soil and the flexible barrier would permit

the sample to remain in vacuum while allowing it to deform under axial stress.

Figure 6.1 shows a section through the chamber as it would appear during sample compaction. Figure 6.2 shows a similar view of the chamber with the sample in a triaxial state of stress.

The chamber was machined from a solid cylinder of aluminum. The overall length was 35.6 cm (14 in.), flange diameters were 24.9 cm (9.8 in.), and the inside diameter was 13.3 cm (5.25 in.) for the lower 15.2 cm (6.0 in.) of the chamber and 11.4 cm (4.5 in.) for the upper 20.3 cm (8.0 in). Aluminum flanges bolted to the top and bottom of the chamber body compressed rubber o-rings to create a vacuum tight seal. Both flanges had holes bored through them radially from which to draw the vacuum. The bottom flange was fabricated with recesses to accept a porous stone and rubber o-ring. Seals on the chamber were designed to contain a vacuum of 10^{-7} torr based on accepted vacuum seal specifications, Roth (1976)

A polished steel sleeve hardened to Rockwell 65 hardness number provided the constraint for the sample during compaction. Hardening was required to prevent the simulant grains from becoming embedded in the sleeve. The length of the sleeve was 20.3 cm (8.0 in.), the inside diameter was 7.62 cm (3.0 in.) and the outside diameter was slightly

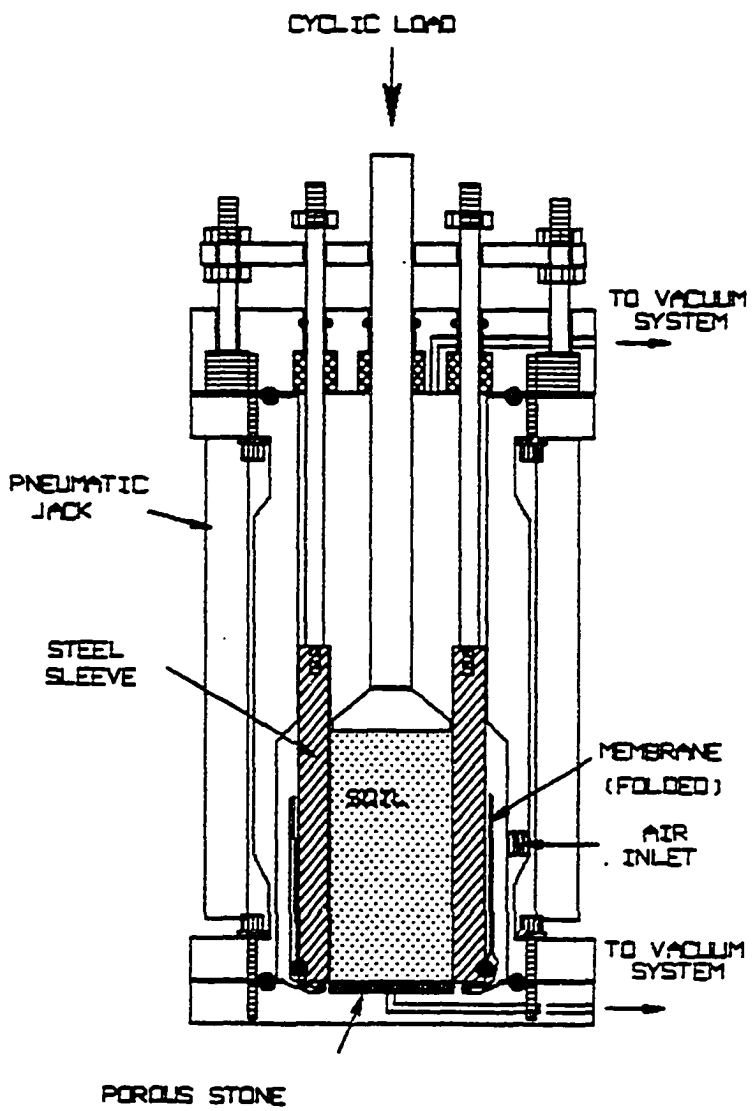

Fig. 6.1 Vacuum Triaxial Chamber: Compaction Mode

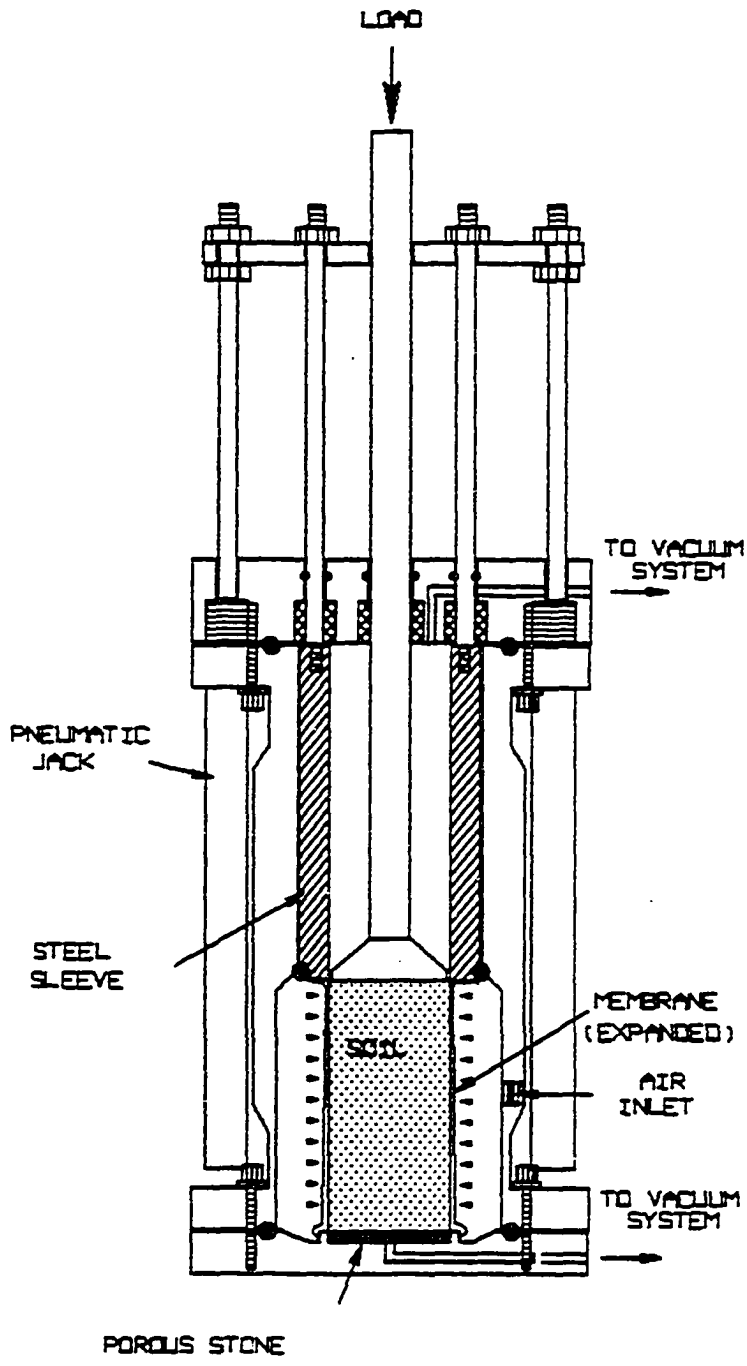

Fig. 6.2 Vacuum Triaxial Chamber: Triaxial Mode

less than 11.4 cm (4.5 in.). As shown in Figure 6.1, the sleeve rested on the bottom flange during sample compaction and was raised until it contacted the top flange during triaxial testing (Figure 6.2).

Two pneumatic rams at diametrically opposite locations outside the chamber body were threaded into the upper flange. The 0.953 cm (0.375 in.) diameter shafts from the rams were linked to two similarly sized 25.4 cm (10.0 in.) long stainless steel shafts. These shafts penetrated the upper flange and were threaded into the top of the steel sleeve within the vacuum chamber. The pneumatic rams each provided a lifting force of 0.33 kN (75 lbs) to raise the steel sleeve from around the soil specimen. In addition to the two shafts linking the sleeve and the rams, the 2.54 cm (1.0 in.) diameter load piston actuator shaft also penetrated the upper flange. These three shafts were surrounded by rubber o-rings within the flange to provide a vacuum seal. The shafts rode in brass bushings which served as bearings to maintain correct alignment during vertical motion.

The flexible barrier which allowed the sample to deform laterally under triaxial stress conditions while providing a vacuum seal consisted of a Soiltest T614 latex rubber triaxial membrane 10.2 cm (4.0 in.) in diameter and 22.9 cm

(9.0 in.) long. One end of the membrane was held by a large rubber o-ring in a 0.46 cm (0.18 in.) groove machined around the bottom of the steel sleeve. The other end of the membrane was attached to the bottom flange in a similar fashion by a smaller o-ring. During sample compaction, while the sleeve was in the down position (Figure 6.1), the membrane was folded against the outside of the steel sleeve in the space between the sleeve and the chamber wall. After compaction, as the sleeve was pulled upward, the membrane unfurled to surround the sample (Figure 6.2).

When the steel sleeve was fully raised the large o-ring holding the membrane to its base contacted the tapered portion of the vessel wall. This effectively isolated the upper region of the vacuum chamber and the evacuated soil sample so that vacuum was maintained while the confining stress was applied. A small port in the lower region of the chamber could now be opened to allow the application of air pressure as the confining stress. Vertical stress, controlled by the MTS testing system described in Section 5.3, could then be applied via the loading piston to the sample.

Prior to beginning the actual testing program, a series of trial tests were conducted to establish some of the operating characteristics of the vacuum triaxial chamber. With a simulant sample in the chamber it was found that 48

hours of pumping were required to reach a vacuum of 1×10^{-4} torr. Thirty-six hours were required to reach 1×10^{-3} torr, 2 hours to reach 1×10^{-2} torr, and about 0.5 hours to reach 1×10^{-1} torr.

With the soil sample removed, a load correction for the friction on the actuator shaft was determined in the following manner: the shaft was slowly moved downward at the rate corresponding to a strain rate of 0.05% per minute on an actual sample. The load required to maintain this rate was 0.11 kN (25 lbs) and this value was subtracted from the loads recorded during actual triaxial testing. To establish a datum from which to measure sample strain during testing, an aluminum cylinder machined to 15.24 +/- 0.003 cm (6.000 +/- 0.001 in.) was placed in the empty chamber. When the loading piston contacted the cylinder and a load of 0.22 kN (50 lbs) was placed on it, the digital readout of voltage from the LVDT (Section 5.3) was recorded. Voltage readings taken during an actual test can be compared to this value to determine sample height and strain.

During the trial tests, it was discovered that the pneumatic rams did not supply sufficient force to lift the steel sleeve from around the sample. However, with the addition of a small amount of upward force the sleeve would rise to the fullest possible extent. The distance the

sleeve could rise was 14.6 cm (5.75 in.) as opposed to the 15.2 cm (6.0 in.) anticipated during design (Figures 6.1 and 6.2). It was assumed that the heat treating process required to harden the steel sleeve caused a mis-alignment of holes into which the lifting shafts were threaded. The mis-alignment was sufficient to cause binding of the shafts as the sleeve was raised to near the top of the chamber.

Because the latex membrane was 2.54 cm (1.0 in.) larger in diameter than the recess that it fastened to on the bottom flange (Figure 6.2), silicon rubber sealant was required around the bottom of the membrane to prevent leakage. The time required for this silicon sealant to cure had to be considered when scheduling tests. It was found that when the membrane was fully extended and the air inlet port opened; the permeability of the membrane caused the vacuum level in the chamber to drop to about 2×10^{-2} torr. The pressure rose to this level regardless of the confining pressure or the initial vacuum in the chamber (as long as it was greater than 2×10^{-2} torr). At vacuum levels lower than 2×10^{-2} torr no leakage occurred.

6.2 Test Procedures

6.2.1 Density/Vacuum/Cyclic Load Tests

Based on conclusions from the pilot study (Section 5.6), only one initial density was considered for this series of tests. This density was 1.552 g/cm^3 and for all practical purposes was the loosest state for the lunar soil simulant. To find the mass of the sample required for these tests, consideration was given to the desired final height of of the sample and the anticipated maximum density after cyclic loading. The desired final height of the specimen was 14.61 cm (5.75 in.) which is the maximum distance that the steel sleeve can be raised. The anticipated maximum density after cyclic loading was 2.04 g/cm^3 based on results from the pilot study. The volume of sample inside the 7.62 cm (3.0 in.) diameter sleeve after compaction would be 666.0 cm^3. When this volume was multiplied by the anticipated maximum sample density the mass of the samples was found to be 1.360 kg. This value was constant for all of the vacuum triaxial testing.

A trial compaction test was conducted in the vacuum triaxial chamber with a cyclic load amplitude varying from 2.22 kN (500 lbs) to 6.67 kN (1500 lbs). It was found that within 5000 cycles the sample density was comparable to the densities achieved under much higher amplitudes after 4000

cycles in the pilot study (Section 5.5). Therefore, this loading program was selected for the compaction study associated with the vacuum triaxial tests. Figure 6.3 shows the loading pattern employed for the compaction phase of the vacuum triaxial tests. It was hoped that by using a lower load, the effects of vacuum on compaction would become more apparent.

Procedures for the tests to study the effects of vacuum level and cyclic load on the density of the lunar soil simulant were essentially the same for samples in the vacuum triaxial chamber as for samples in the pilot study chamber (Section 5.4). The exceptions are those noted above and that the compaction was carried out in a hardened steel sleeve which would deform much less than the teflon liner of the pilot study chamber. Simulant to be tested in vacuum conditions was loaded directly into the chamber from an oven where it had been heated to 130 $^{\circ}$ C for a minimum of 36 hours. Samples to be tested at atmospheric pressure were allowed to cool to room temperature prior to being loaded into the chamber. All samples were sifted into the steel sleeve so that they were in the loosest possible state. Initial sample height was approximately 19.3 cm (7.58 in.). Before evacuation began, the loading piston was lowered until it just contacted the top of the loose samples (based on the calibration datum, Section 6.1). When the desired

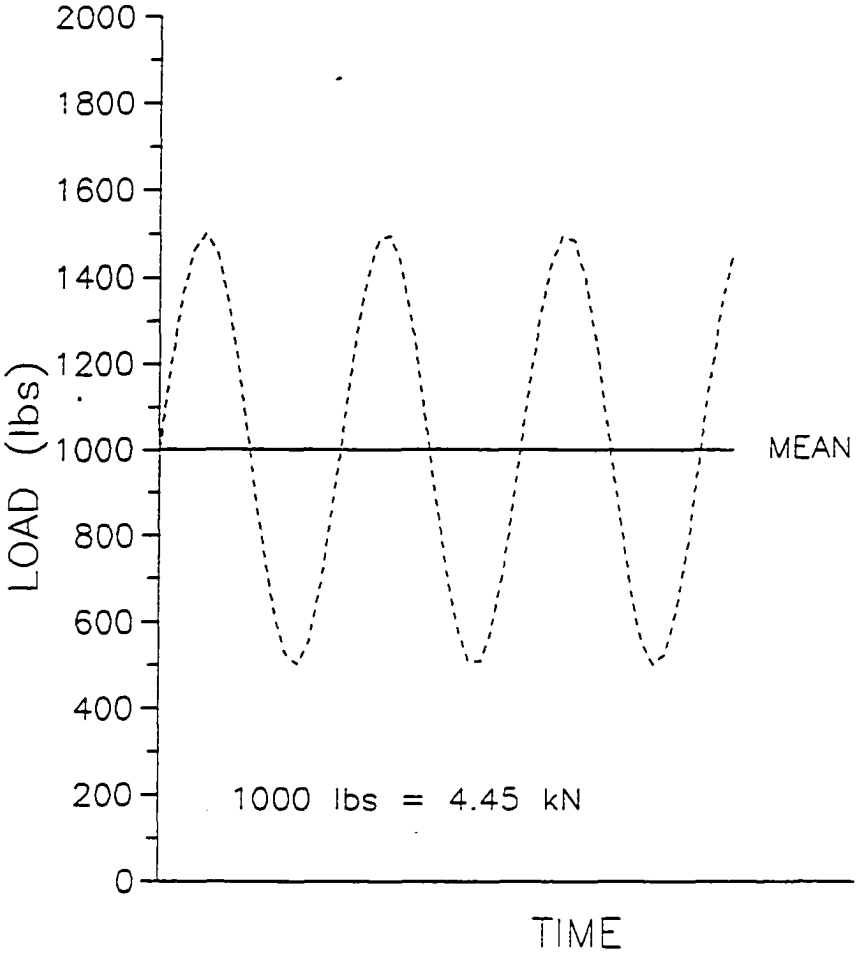

Fig. 6.3 Cyclic Load Pattern: Vacuum Triaxial Tests

vacuum level was reached, it was maintained for a minimum of 12 hours and a maximum of 14 hours before cyclic loading commenced.

During the compaction process, deformation readings were recorded at zero load, and at the mean cyclic load of 4.45 kN (1000 lbs) (Figure 6.3) for the first, second, fifth, and tenth cycles. Subsequent readings were recorded every 10 cycles up to 50 cycles, then at 100 cycles, and every 100 cycles thereafter. The samples underwent 5000 cycles of loading at which point deformation per 100 cycles was less than 0.003 cm (0.001 in.). These tests were repeated three times at vacuum levels of 760 torr, 0.5 torr, 0.05 torr, and 0.005 torr.

6.2.2 Constrained Compression Tests

After the lunar soil simulant samples had been compacted to the final density, and prior to removal of the steel sleeve for triaxial testing, the samples were tested in constrained compression. Each specimen experienced two complete cycles of loading and unloading.

For the first load cycle, the samples were loaded to 2.05 MPa (297 psi) or 140% of the maximum stress that had occurred during the compaction process. The load was applied very slowly and deformations were recorded at

approximately 0.21 MPa (30 psi) intervals beginning at zero, and including 1.46 MPa (212 psi) and 2.05 MPa (297 psi). At each loading step, the stress was held constant and the strain was allowed to increase until it slowed to a strain rate of 0.005% per minute. When a load of 2.05 MPa (297 psi) was reached and the strain recorded, the sample was slowly unloaded to zero stress and deformation was recorded in the same manner as during loading.

The second loading cycle was conducted similarly except that the maximum stress was 2.73 MPa (396 psi) or 187% of the maximum cyclic load. During the unloading portion of this cycle, the stress was reduced to 0.39 MPa (57 psi) instead of zero. The sample was then reloaded slowly to 2.14 MPa (311 psi) to complete the test. This test was repeated three times at each of the four vacuum levels under consideration (Section 6.2.1).

6.2.3 Vacuum Triaxial Compression Tests

Upon completion of the constrained compression tests, the vacuum triaxial chamber was re-configured as shown in Figure 6.2 by lifting the steel sleeve from around the sample and pulling the membrane into place. In order for the vacuum within the chamber to remain at the desired level; and to prevent damage to the compacted lunar soil simulant, the procedures listed below were followed.

1. The vertical load on the sample was set to zero and the LVDT voltage was recorded.
2. Hydraulic pressure to the MTS loading frame was shut off. This locked the vertical load piston in place at the top of the sample.
3. The vertical load was recorded. It usually read about 0.11 kN (25 lbs).
4. Air pressure of 0.52 MPa (75 psi) was applied to the pneumatic rams. The steel sleeve was forced up to the fullest possible extent and the distance it rose was recorded.
5. The air inlet port was opened allowing air at atmospheric pressure, 0.10 MPa (15psi), to surround the sample.
6. The vertical load cell reading was recorded. It usually showed about 0.29 kN (65 lbs).
7. The LVDT voltage was recorded; it usually showed a slight negative strain, indicating expansion of the sample.
8. The 406 Controller was switched to low load scale and the hydraulic pressure to the load frame was restored. This caused the load on the sample to drop to about 0.11 kN (25 lbs)
9. The vertical load on the sample was recorded.
10. The LVDT voltage was recorded; it indicated an

increase in negative strain.

11. The strain was increased at 0.05% per minute by slowly increasing the load on the sample. Load and deformation readings were recorded for every 0.05% of strain. For samples tested at a confining stress of 0.10 MPa (15 psi), loading continued in this fashion until a peak load was observed and the strain had exceeded 5%.

12a. For samples tested at higher confining pressures, the vertical load was increased as in step 11 until the vertical stress equalled the confining stress.

12b. The air pressure line was attached to the air inlet port and the confining pressure was increased by 0.03 MPa (5 psi)

12c. Steps 12a and 12b were repeated until the desired confining stress was reached.

13. The sample was loaded as in step 11 until failure occurred.

This process resulted in an initial stress history for the sample which is different from that in a conventional triaxial compression test where ($\sigma_1 > \sigma_2 = \sigma_3$). This is because with the present setup it is not possible to apply the confining stress in such a way that an equal all around stress results simultaneously. Consequently, the initial state of stress, before the shear loading commences, is

anisotropic and not hydrostatic. Vacuum triaxial tests were conducted in this manner for confining stresses of 0.10 MPa (15 psi), 0.14 MPa (20 psi), and 0.17 MPa (25 psi) at vacuum levels of 0.5 torr, 0.05 torr, and 0.005 torr.

To control the rate of strain of the samples the load was increased manually while timing the deformation with a stop watch. No difficulty was encountered in maintaining a strain rate of 0.05% per minute when the MTS 406 controller was set to the high resolution/low load scale (0 kN - 4.4 kN), (0 lbs - 1000 lbs).

Confining stresses less than 0.10 MPa (14.7 psi), atmospheric pressure, were not possible without some modification to the chamber. Because there was no control valve at the air inlet port; and no gage to measure vacuum at the port, there was no means to restrict the air entering the chamber and thus create a confining stress less than atmospheric pressure. When a sample was tested at a confining stress of 0.20 MPa (30 psi) the vertical load required to fail the sample exceeded the high resolution scale of the MTS 406. At the higher load scale (0 kN - 44 kN), (0 lbs - 10000 lbs) adequate manual control of the strain rate was not possible. For this reason the greatest confining stress used was 0.17 MPa (25 psi). For soil at a density of 2.00 g/cm^3 this would be equivalent to a depth of about 1.5 m (5 ft) beneath the lunar surface.

6.2.4 Conventional Triaxial Compression Tests

A series of three conventional triaxial tests was conducted to provide baseline data with which to compare the results of the vacuum triaxial tests. These tests were performed in a conventional triaxial cell with water pressure as the confining stress. High sample density was achieved by compacting the oven dried lunar soil simulant in a 6.35 cm (2.5 in.) diameter mold. All samples had an initial height of 12.70 cm (5.0 in.) and sample densities were comparable to the final densities of the samples tested in vacuum. Confining stresses were 0.10 MPa (15 psi), 0.14 MPa (20 psi), and 0.17 MPa (25 psi) and the tests were conducted undrained, although this was irrelevant because no moisture was present in the samples.

6.3 Results of Vacuum Triaxial Tests

6.3.1 Density/Vacuum/Cyclic Load Tests

Initial and final densities resulting from selected numbers of cycles of loading at four vacuum levels are listed in Table 3. Three tests were run at each vacuum level. Sample density was calculated in the manner described in Section 5.5. In order to better depict the effect of the first 100 cycles of loading on the final density of the lunar soil simulant, Figure 6.4 shows the

Table 3

Simulant Densities for Selected Numbers of Cycles of Loading : Vacuum Triaxial Tests

Vacuum Level (torr)	Density (g/cm^3)					
	No. of Cycles					
	0	1	10	100	1000	5000
760	1.552	1.947	1.955	1.962	1.974	1.985
	1.552	1.940	1.947	1.955	1.970	1.983
	1.552	1.940	1.947	1.957	1.967	1.978
5×10^{-1}	1.552	1.958	1.967	1.979	2.000	2.020
	1.552	1.964	1.971	1.985	2.007	2.029
	1.552	1.968	1.975	1.987	2.008	2.028
5×10^{-2}	1.552	1.957	1.963	1.974	1.992	2.010
	1.552	1.946	1.955	1.965	1.985	2.007
	1.552	1.965	1.971	1.984	2.005	2.025
5×10^{-3}	1.552	1.947	1.954	1.962	1.978	1.993
	1.552	1.939	1.947	1.958	1.976	1.993
	1.552	1.951	1.958	1.969	1.989	2.009

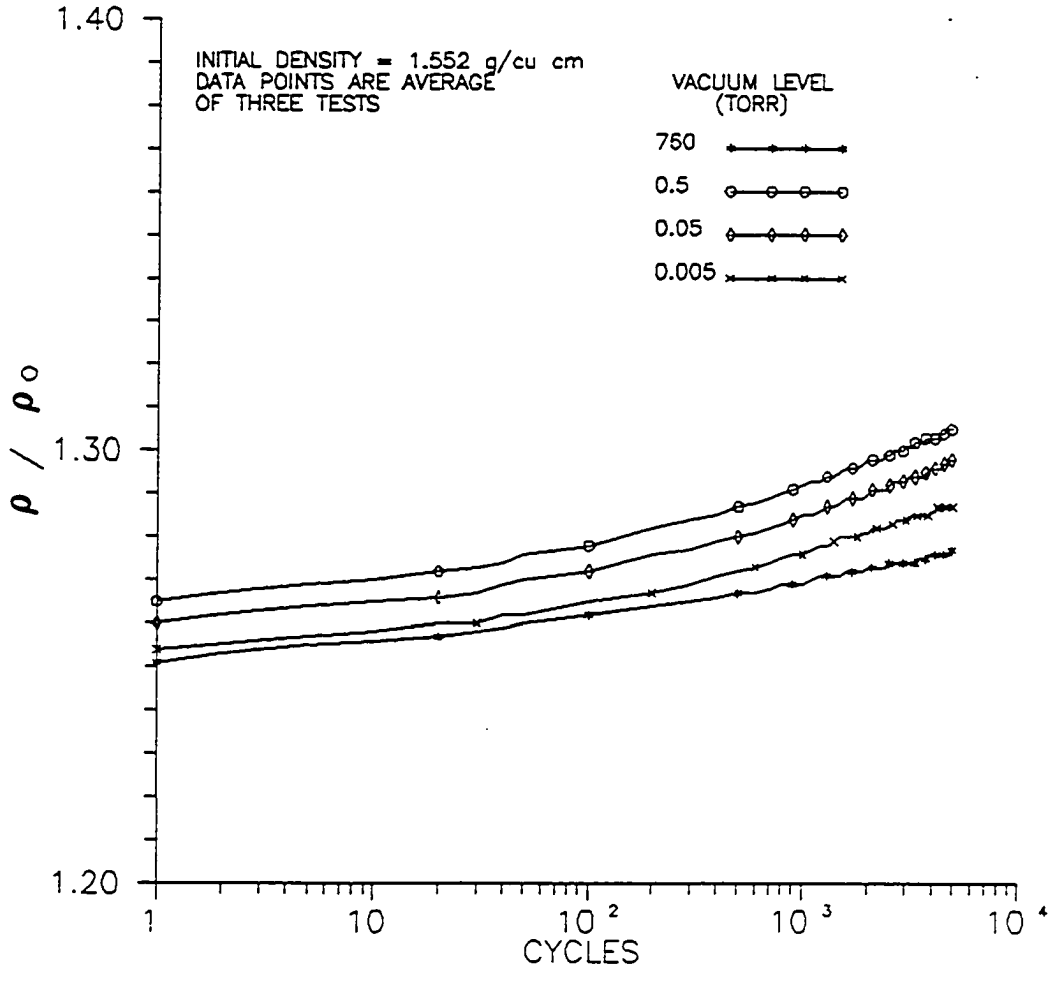

Fig. 6.4 Density Ratio vs. Number of Cycles

number of cycles on a horizontal logarithmic scale plotted against the ratio of sample density, ρ , to initial sample density, ρ_0 (1.552 g/cm^3), on a vertical linear scale.

As indicated in Table 3 and Figure 6.4, the highest densities were reached in the vacuum of 0.5 torr and the lowest densities occurred at 760 torr. Close examination of Figure 6.4 reveals that for high numbers of cycles the rate of increase in density, i.e., the slope of the density ratio vs. cycles curve, is noticeably smaller for samples compacted at 760 torr than for samples compacted in vacuum.

In Figure 6.5, the ratio of compacted density, ρ, to initial density, ρ_0, is plotted against vacuum level for selected numbers of cycles of loading. The graph shows that at any number of cycles, the samples at 0.5 torr have the highest density ratio while the samples at 760 torr have the lowest ratio. The samples compacted at 0.05 torr and 0.005 torr have density ratios only slightly higher than the samples at 760 torr for any number of cycles.

6.3.2 Constrained Compression Tests

The stress-strain curves for the constrained compression tests conducted at 760 torr, 0.5 torr, 0.05 torr and 0.005 torr are shown in Figure 6.6. Each data point represents the average value of strain for the three tests run at each

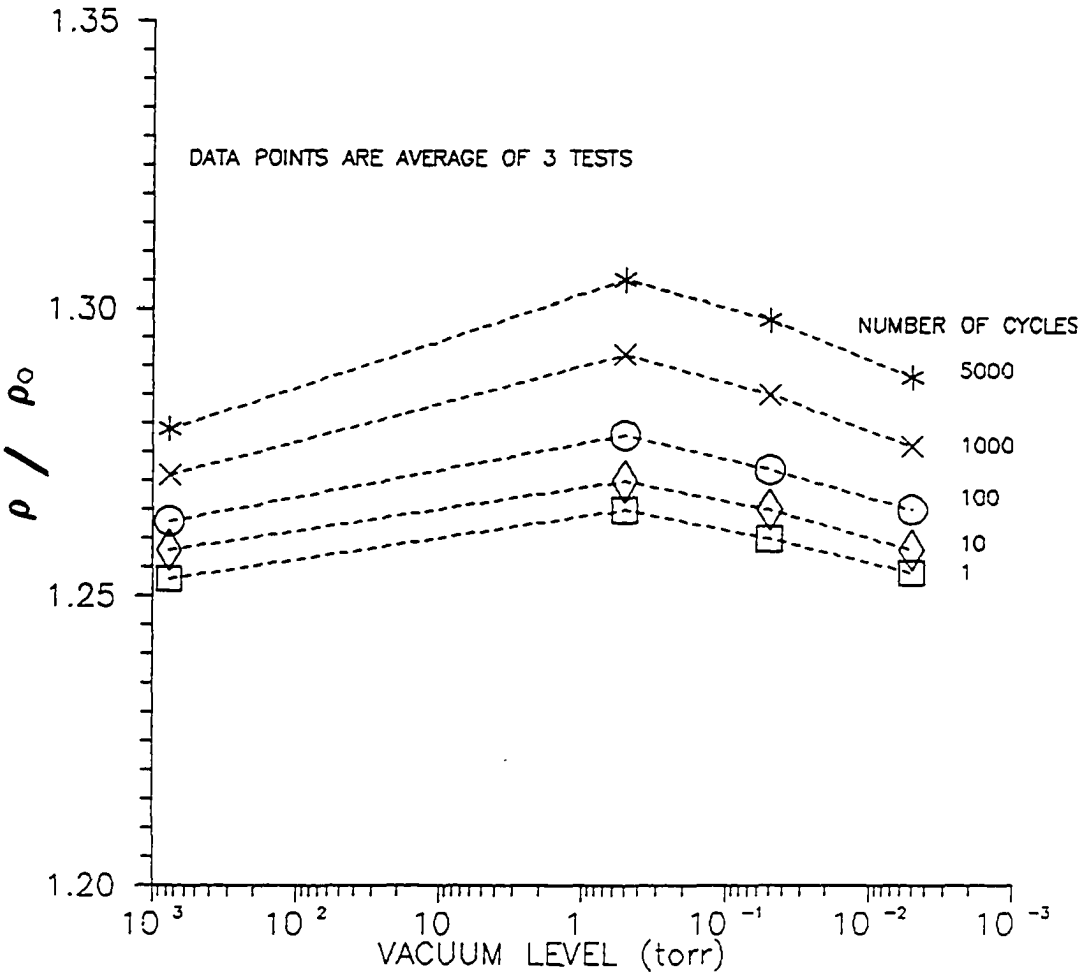

Fig. 6.5 Density Ratio vs. Vacuum Level for Selected Numbers of Cycles of Loading

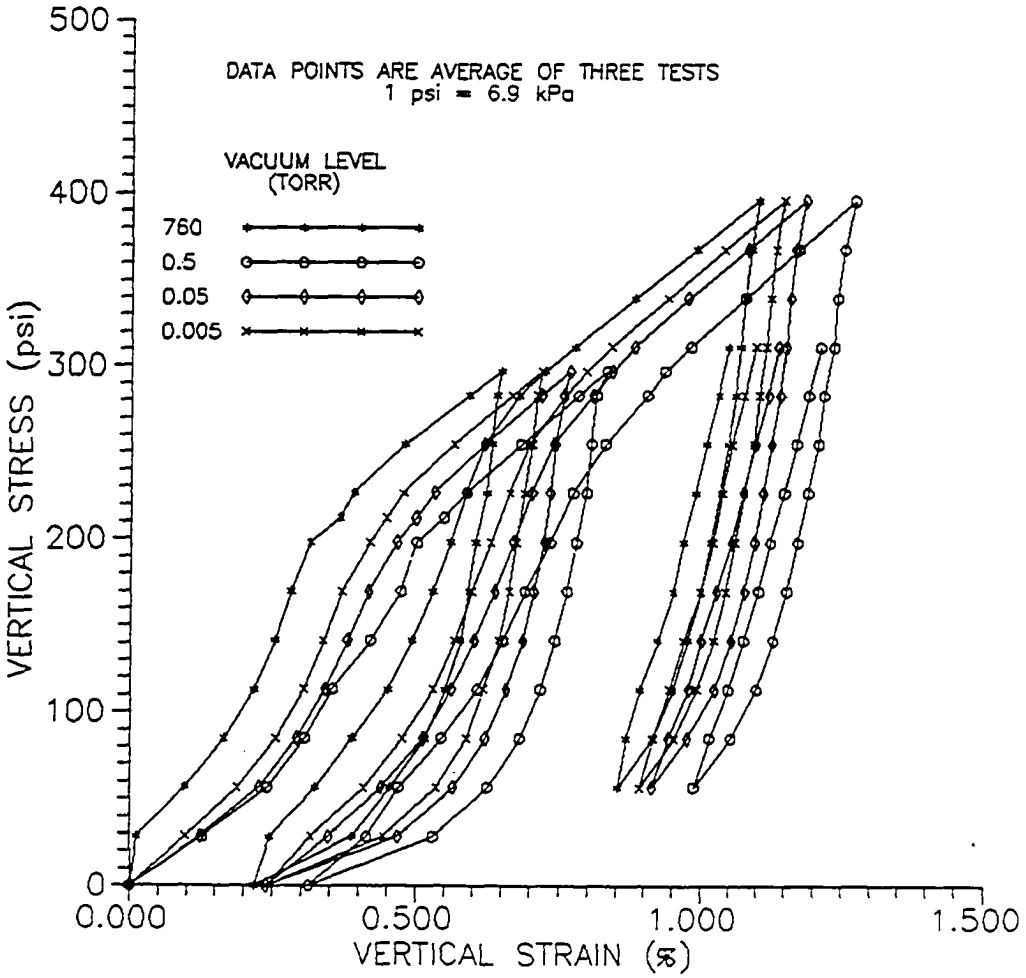

Fig. 6.6 Stress vs. Strain for Constrained Compression Tests

vacuum level. To find virgin compression moduli for stresses in excess of those previously imposed on the samples; that is, the maximum cyclic stress, 2.05 MPa (297 psi), the slopes of the curves for increasing stress between stresses of 2.05 MPa (297 psi) and 2.73 MPa (396 psi) were determined. This value, E_C, was calculated as the difference in stress between the end points of this portion of the curve divided by the corresponding change in strain.

A recompression or unloading modulus, E_R, was calculated for each test in a similar manner by determining the initial slope of the unloading curves for the second loading cycle. The stress range considered was from the maximum stress, 2.73 MPa (396 psi), to the stress level where the unloading curve became nonlinear, 1.95 MPa (283 psi). Results of these calculations are presented in Table 4 and a plot of average E_C vs. vacuum is shown in Figure 6.7.

The highest average value of E_C was for samples compacted at 0.5 torr. The lowest average value was for samples compacted at 760 torr. Values of E_R followed a different pattern: the samples tested at 760 torr had the highest average unloading modulus while those tested at 0.5 torr had the lowest average value of E_R. For samples tested at

Table 4

Values of Constrained Modulus

for Four Vacuum Levels

Vacuum Level (torr)	E_C = Virgin Compression E_R = Re-compression		
	Test No.	E_C (psi)	E_R (psi)
760	1	256	2572
	2	*	*
	3	269	3233
0.5	1	292	2096
	2	307	2096
	3	290	2096
0.05	1	279	2572
	2	302	2572
	3	287	2572
0.005	1	281	2572
	2	296	2572
	3	272	2572

* Data unavailable

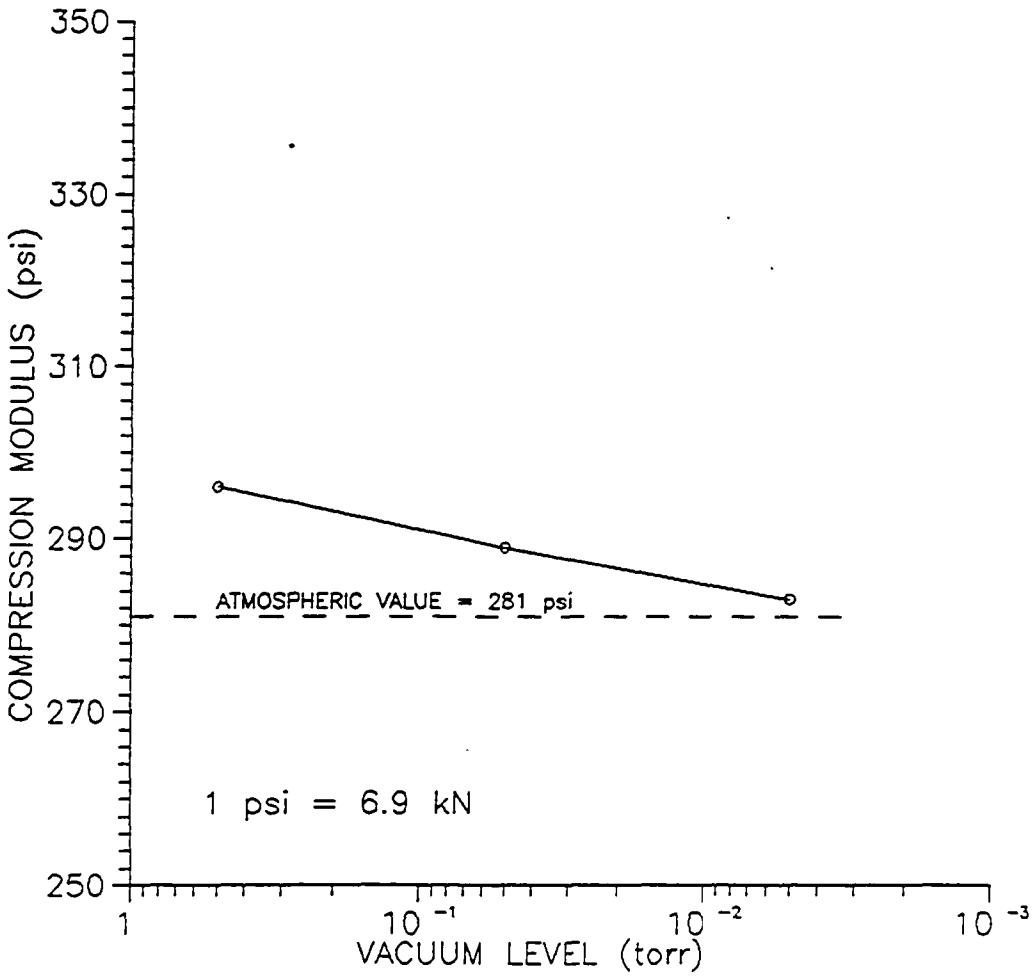

Fig. 6.7 Average Virgin Compression Modulus vs. Vacuum

0.05 torr and 0.005 torr the average values of E_R were identical.

6.3.3 Vacuum Triaxial Compression Tests

Stress-strain curves for the vacuum triaxial compression tests are shown in Figures 6.8 through 6.10. Included on these figures is a graph showing the initial and subsequent stress paths for each sample. Here the loading and unloading which occurred at the start of each test is portrayed in p-q space where:

$$p = (\sigma_v + 2(\sigma_h))/3$$

$$q = (\sigma_v - \sigma_h)$$

σ_v = vertical stress and

σ_h = radial confining stress

The figures show that as the confining stress, σ_h, increased the value $(\sigma_v - \sigma_h)$ at failure also increased.

When the stress-strain curves for a single confining stress at three different vacuum levels are plotted on the same axes as in Figures 6.11 through 6.13, the curves show small variation of failure stress, $(\sigma_v - \sigma_h)_f$, for the vacuum levels considered.

The secant modulus of elasticity was calculated for each vacuum triaxial test. This modulus is defined as the slope

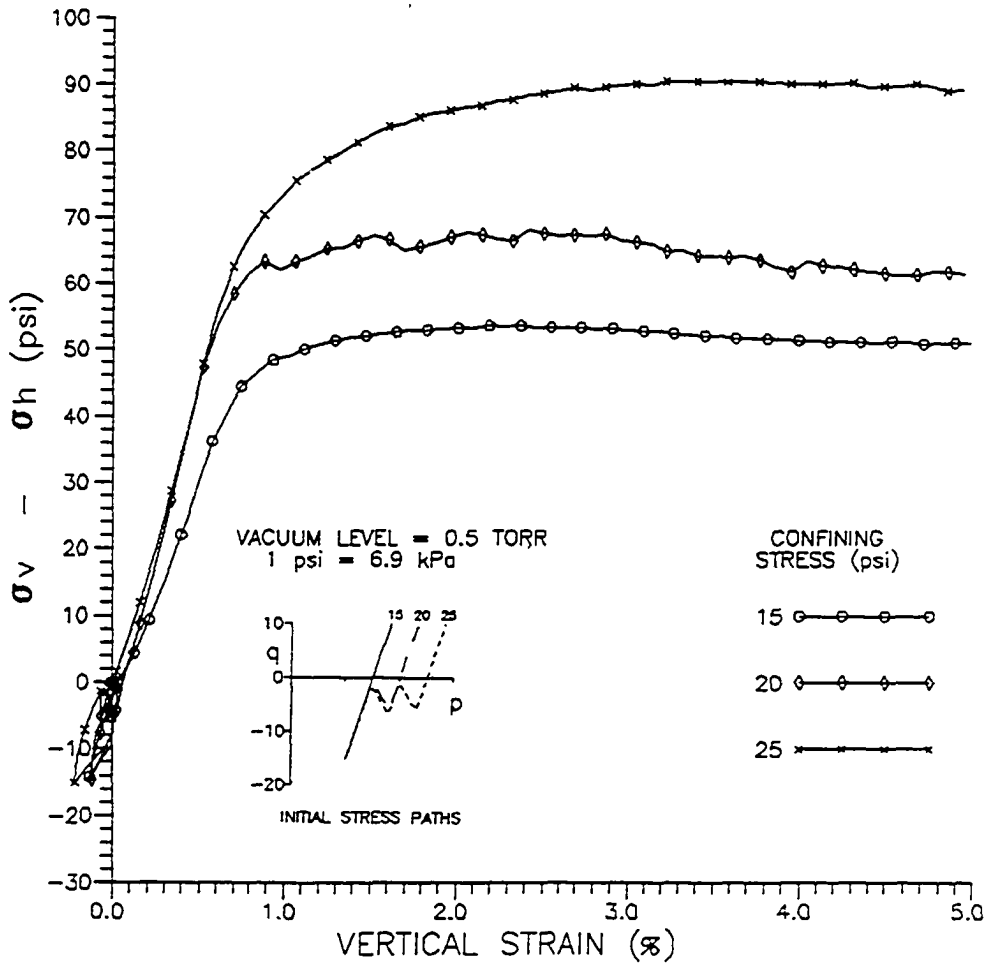

Fig. 6.8 Stress vs. Strain for Vacuum Triaxial Tests

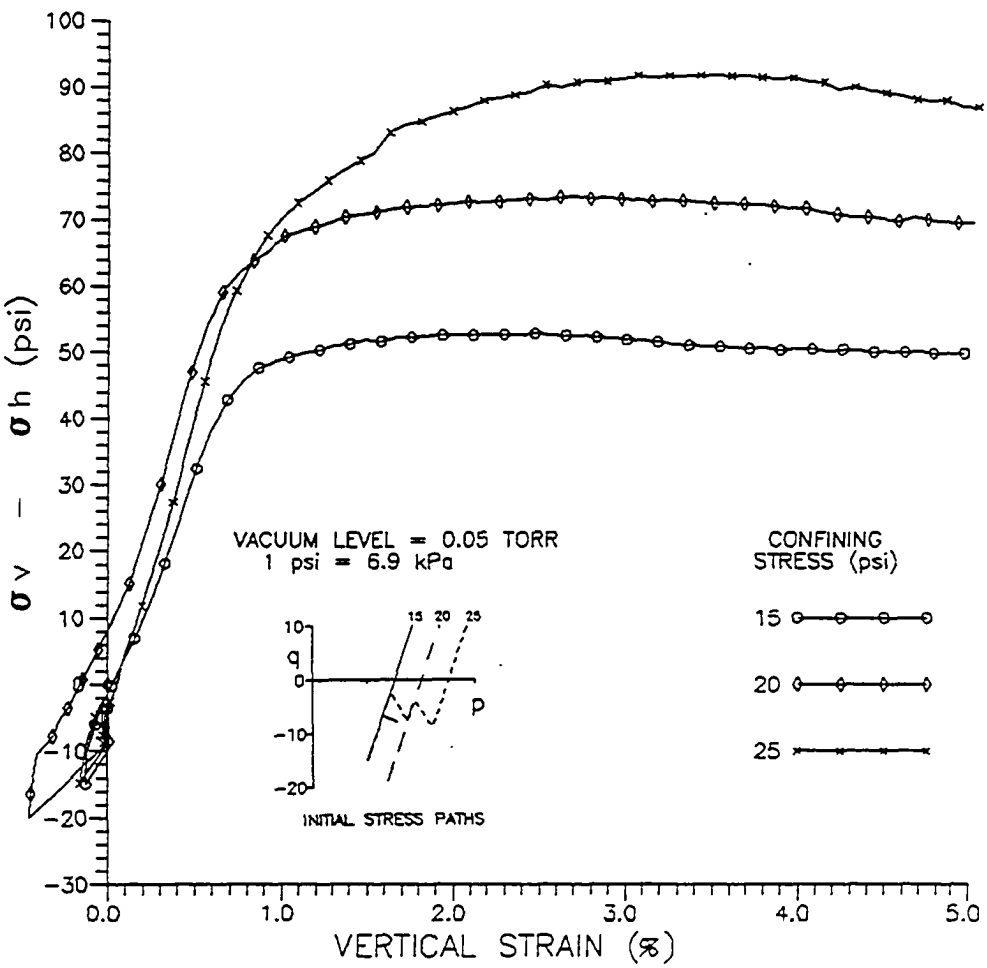

Fig. 6.9 Stress vs. Strain for Vacuum Triaxial Tests

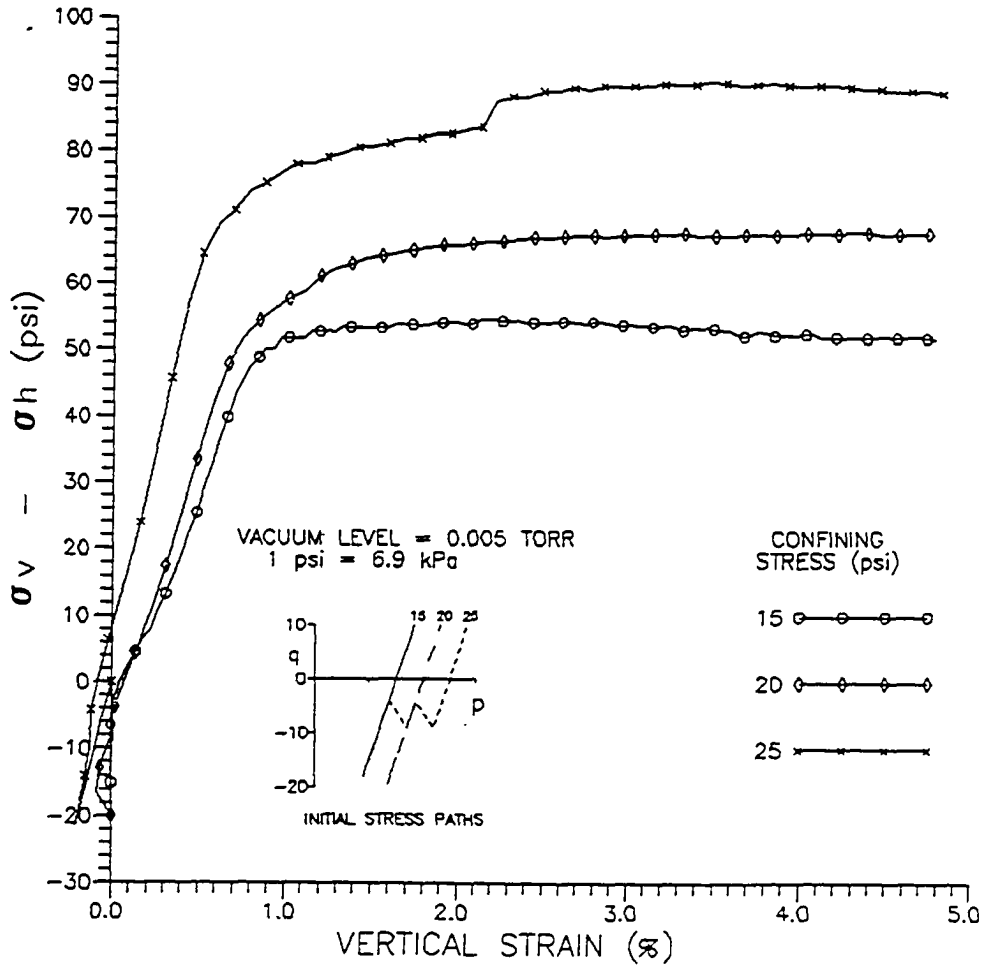

Fig. 6.10 Stress vs. Strain for Vacuum Triaxial Tests

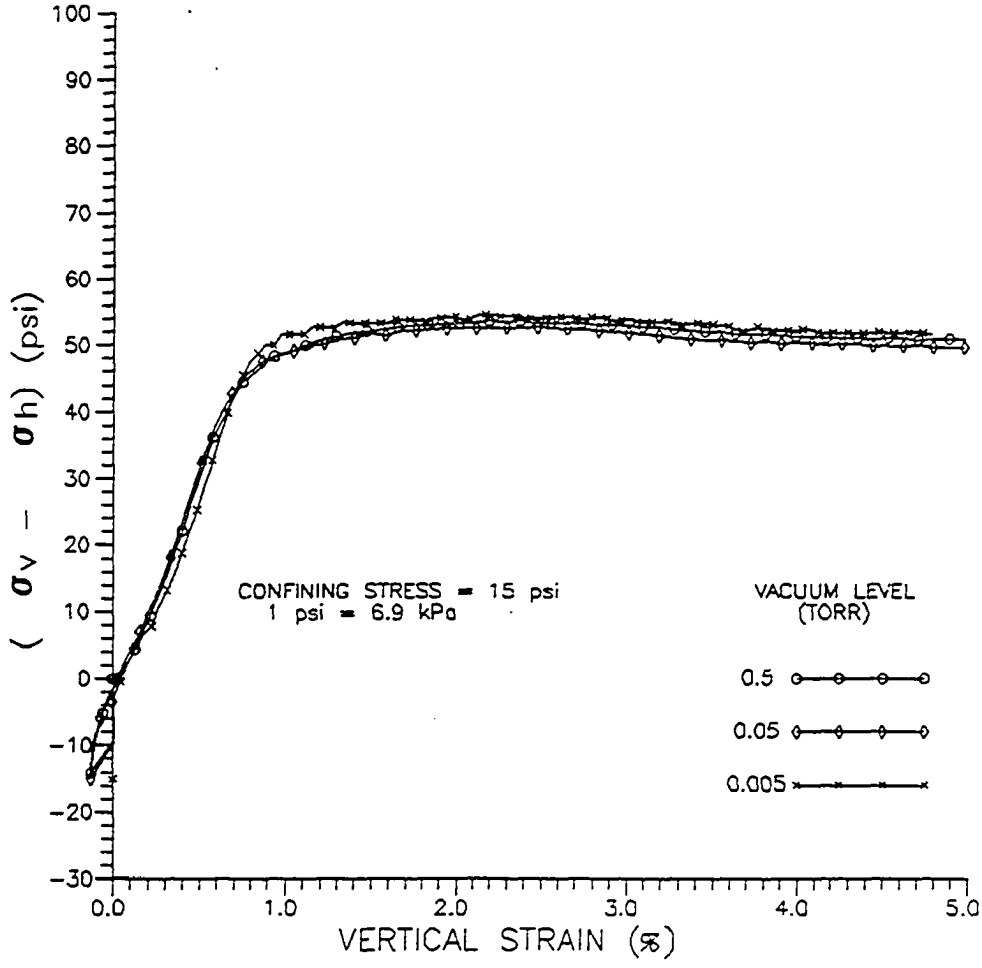

Fig. 6.11 Stress vs. Strain for Vacuum Triaxial Tests

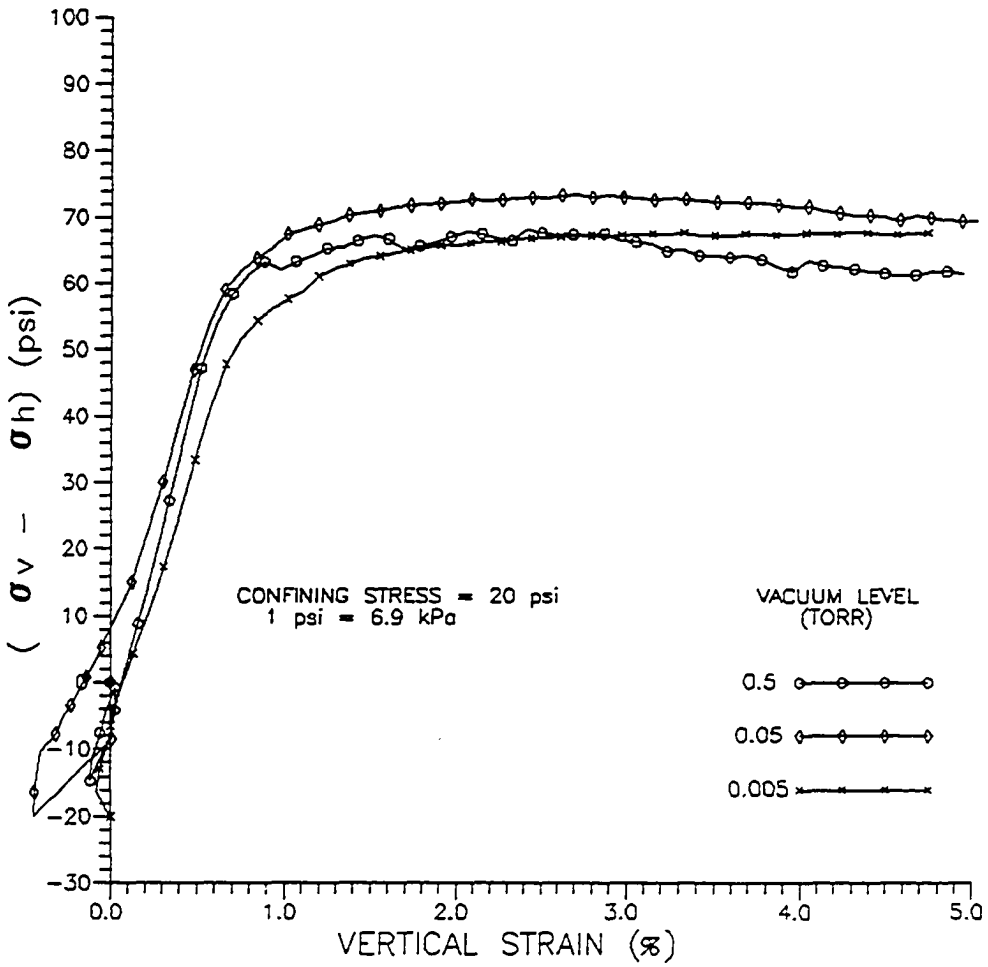

Fig. 6.12 Stress vs. Strain for Vacuum Triaxial Tests

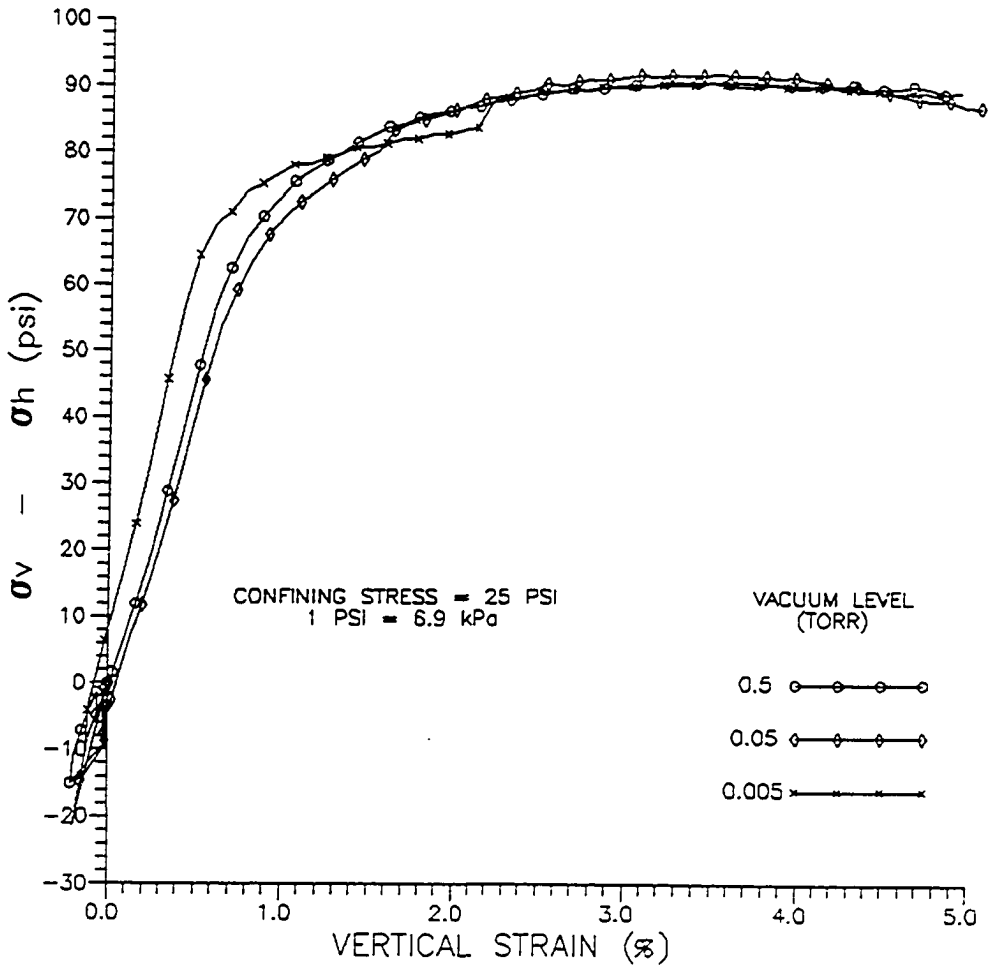

Fig. 6.13 Stress vs. Strain for Vacuum Triaxial Tests

of a straight line drawn on the stress-strain curve from the point of zero stress to some predetermined stress level, Holtz and Kovacs (1981). For this analysis the predetermined stress level was chosen as 50% of the maximum stress. Due to the stress-strain conditions at the onset of these tests, the strain at the point where $(\sigma_v - \sigma_h) = 0$ was not zero. The secant modulus, E_{50}, was calculated as 50% of the failure stress divided by the difference between the strain at 50% of the failure stress and the strain at zero stress. A plot of E_{50} vs. σ_h is shown in Figure 6.14 where a best fit straight line was drawn through the plotted points for each of the three vacuum levels. For all tests the value of E_{50} tended to increased as σ_h increased.

Figures 6.15 through 6.17 depict the results of the vacuum triaxial tests plotted as Mohr's circles. The Mohr-Coulomb failure envelope was drawn as a line tangent to these circles. At all vacuum levels, the angle Φ that this tangent made with the horizontal was approximately 39° and the intersection of the line with the vertical τ axis was very close to zero. Table 5 lists the pertinent values derived from the results of the vacuum triaxial tests. Results from the conventional triaxial compression tests are also included.

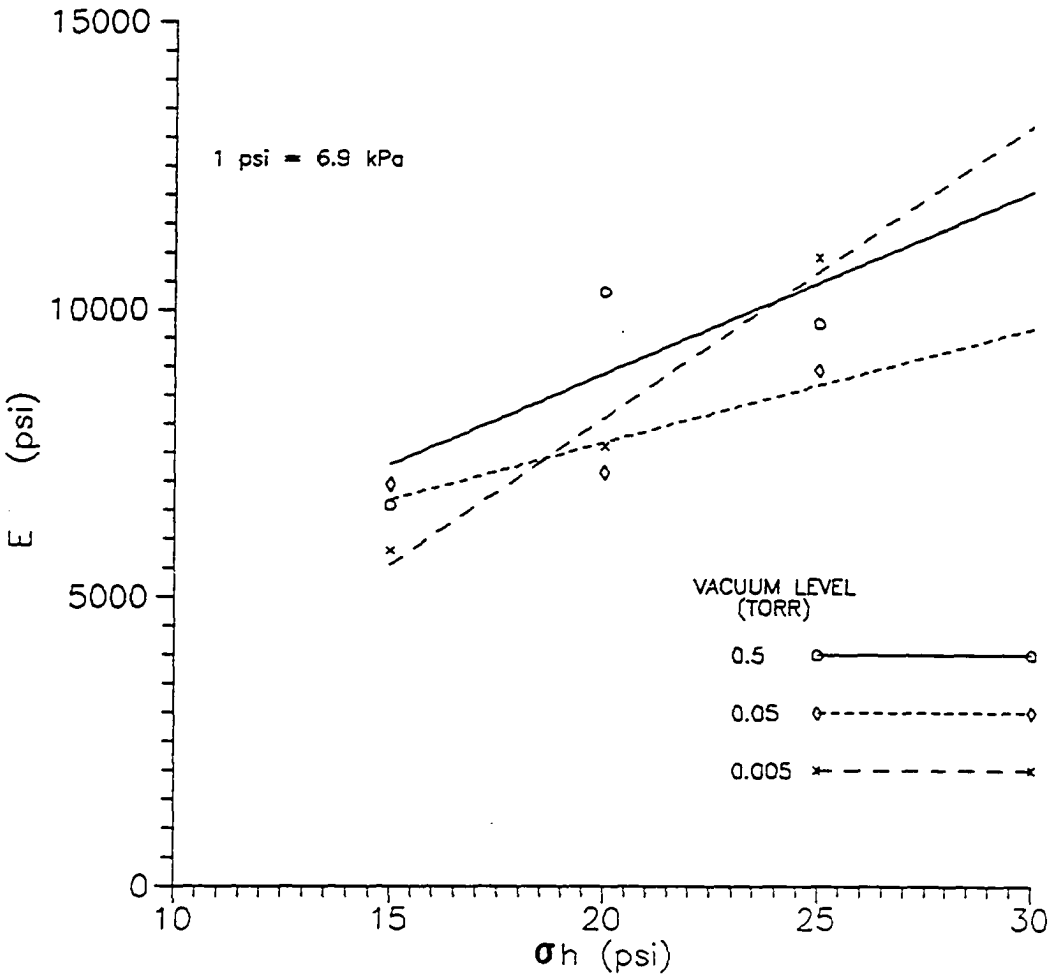

Fig. 6.14 Secant Modulus vs. Confining Stress

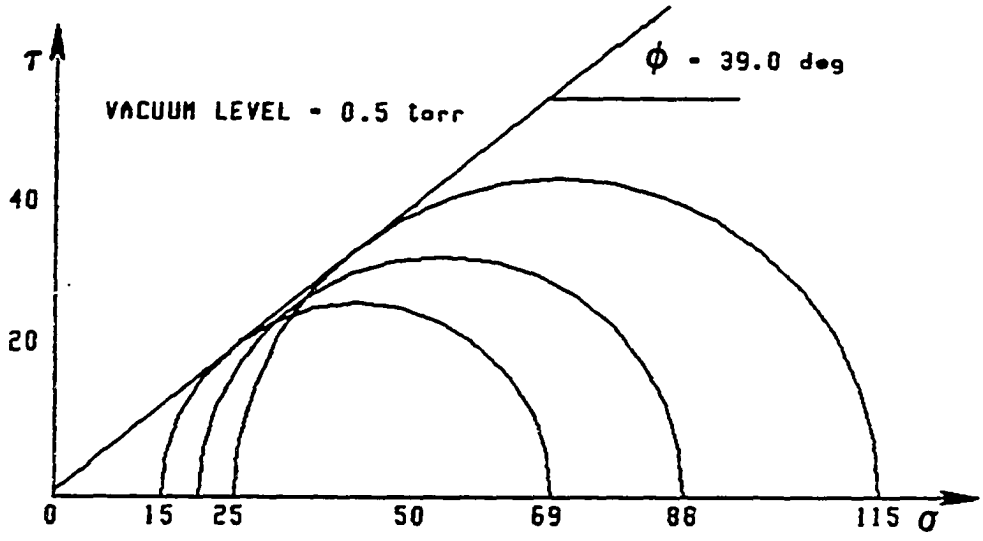

Fig. 6.15 Mohr-Coloumb Envelope for Vacuum Triaxial Tests

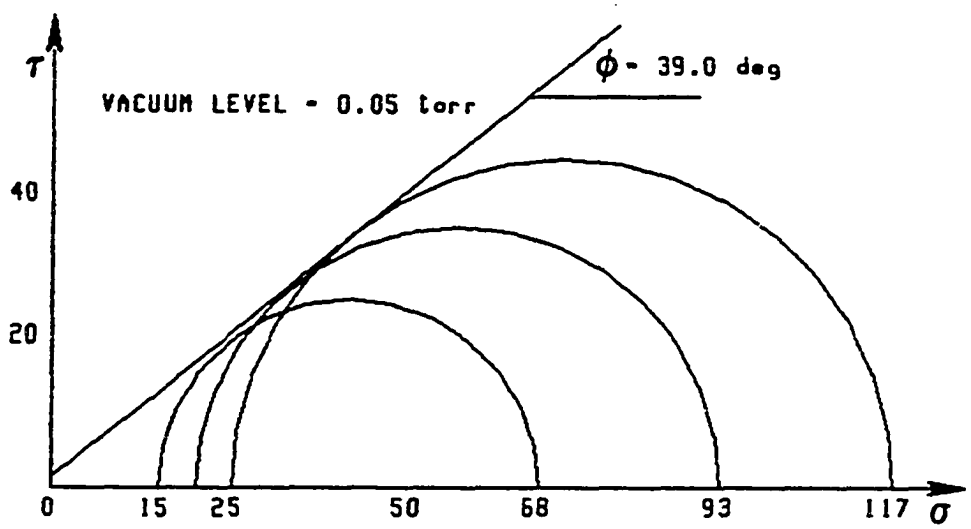

Fig. 6.16 Mohr-Coloumb Envelope for Vacuum Triaxial Tests

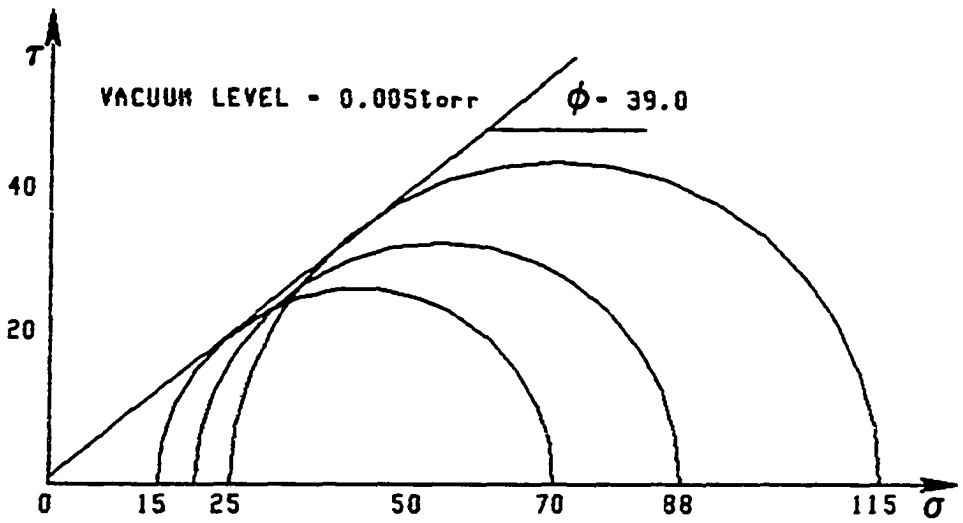

Fig. 6.17 Mohr-Coloumb Envelope for Vacuum Triaxial Tests

Table 5

Results of Triaxial Compression Tests

for Four Vacuum Levels

Vacuum Level (torr)	σ_h = Confining Stress $\sigma_f = (\sigma_v - \sigma_h)$ at failure E_{50} = Secant Modulus		
	σ_h (psi)	σ_f (psi)	E_{50} (psi)
760	15	89	2207
	20	118	3073
	25	132	2996
0.5	15	54	6585
	20	68	10303
	25	90	9755
0.05	15	53	6944
	20	73	7157
	25	92	8941
0.005	15	55	5808
	20	68	7614
	25	90	10905

6.3.4 Conventional Triaxial Compression Tests

Stress-strain plots for the conventional triaxial compression tests are shown in Figure 6.18. The secant modulus for each of these tests was computed in the same manner as for the vacuum triaxial tests. For these three tests, the log of E_{50} was plotted against the log of the ratio of σ_h to sample density, ρ . This was done in an attempt to derive an equation to characterize the relationship between E_{50} and the stress-density ratio for the lunar soil simulant. A best-fit straight line was drawn on the plot (Figure 6.19). The slope of this line was 0.581 and it intersected the E_{50} axis at a value of 2.011.

A Mohr's circle plot for the three conventional triaxial tests is shown in Figure 6.20. The tangent line representing the Mohr-Coulomb failure envelope was at an angle Φ of 39.7° with the horizontal and it intersected the τ axis at a value of 55 kPa (8 psi).

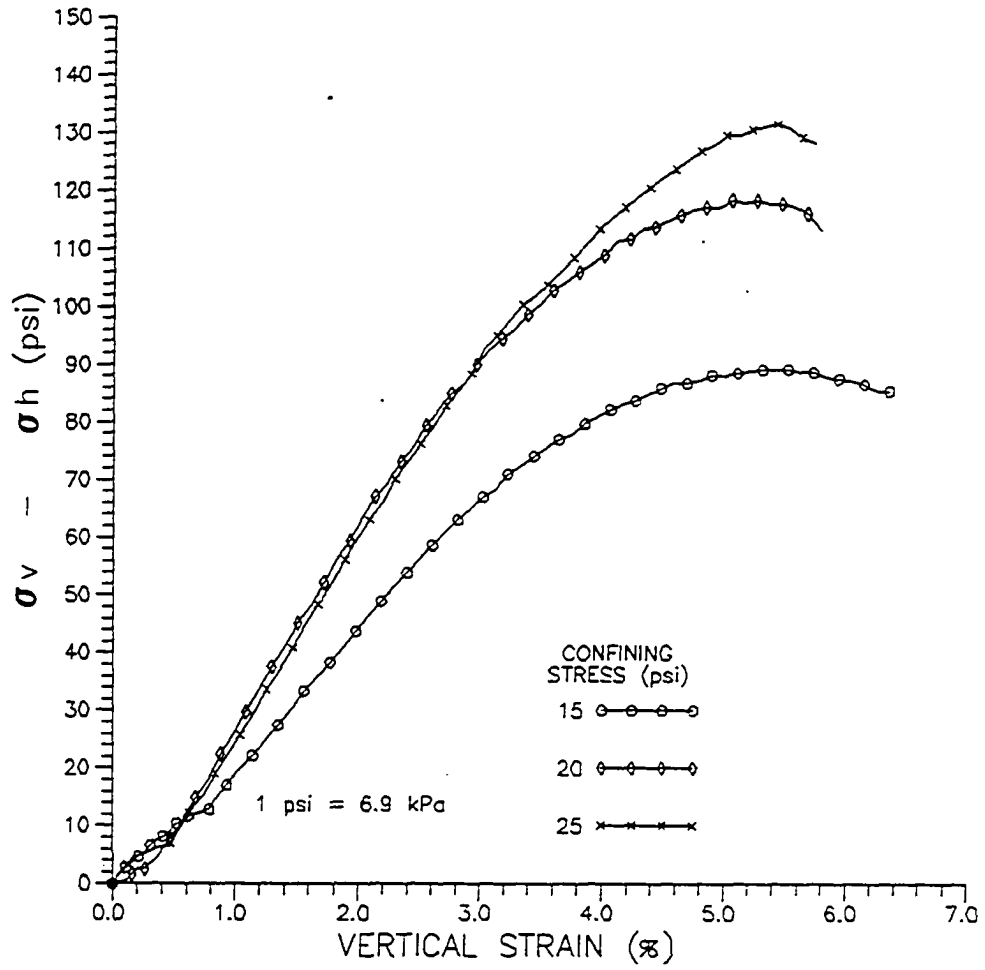

Fig. 6.18 Stress vs. Strain for
Conventional Triaxial Tests

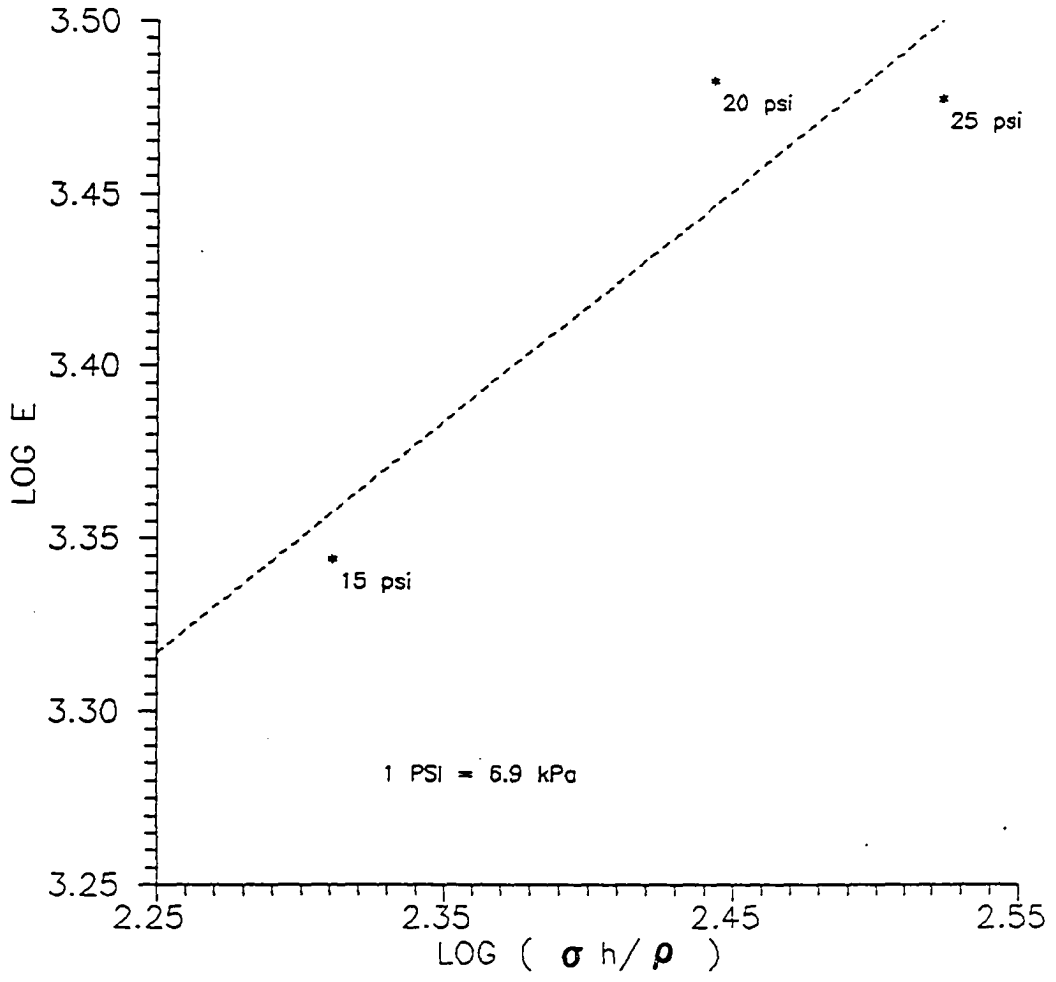

Fig. 6.19 Log (E_{50}) vs. Log (σ_h / ρ)

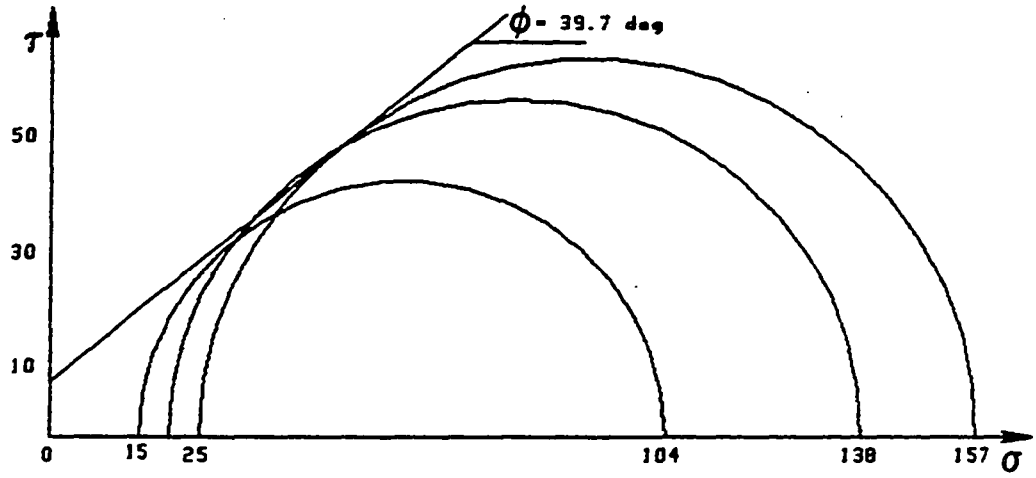

Fig. 6.20 Mohr-Coloumb Envelope for Conventional Triaxial Tests

6.4 Analysis and Conclusions

Results of the density/cyclic load tests show only a slight difference in density for samples compacted at different vacuum levels for any number of cycles. The low final densities observed for samples compacted in atmosphere and the decrease in final density for samples compacted at pressures less than 0.5 torr suggests the existence of an "optimum" vacuum level for compaction in low vacuum (Figure 6.5). This corresponds well with the similar observations of Vey and Nelson (1965) wherein the porosity of lunar soil simulants deposited under vacuum was at a minimum at low vacuum levels. The observed difference in slopes between the density ratio/cycles curves for samples compacted in vacuum (Figure 6.4) and the curve for those samples compacted in air leads to the conclusion that samples compacted in air achieve a maximum density with fewer applications of cyclic load than do samples compacted in vacuum. It may be that water and gas molecules adhering to the surfaces of particles exposed to atmospheric moisture assist the compaction process by reducing friction between particles. In addition, the low density achieved by the sample compacted at 760 torr may be a result of air voids trapped between the particles.

The constrained modulus in virgin compression, E_c, was

more influenced by sample density than by vacuum level. The highest modulus was observed for the sample with the highest density (Figures 6.5 and 6.7). This is the type of behavior to be expected from a soil under these loading conditions, Bowles (1988). The trend in the values of E_R did not follow the predicted pattern in that the lowest unloading modulus corresponded to the samples with the highest density. However, most of the data in Table 4 indicates that there was only one value for E_R independent of vacuum level: 17.7 MPa (2572 psi). This is consistent with the calculated values of E_C which are within a very small range.

At the vacuum levels considered in this investigation, no significant difference in the stress-strain-strength behavior of the lunar soil simulant under triaxial stress conditions was observed. The simulant responded to increases in confining stress with an increase in compressive strength (Figures 6.8, 6.9 and 6.10). In addition, an increase in secant modulus also occurred with an increase in confining stress. This is the expected behavior for a dense sand under these loading conditions and the values of E_{50} are consistent with values typically reported for this soil type, Bowles (1988).

The angle of internal friction, Φ , for all vacuum and conventional triaxial tests was essentially the same

(Figures 6.15, 6.16, 6.17, and 6.20). The vacuum tests showed a very slight value for cohesion and the cohesion for the conventional tests was measurable. Because the variation in confining stress was so small from one test to another; and because even the largest confining stress was small by most standards, the Mohr-Coulomb failure envelope was not linear for these tests as it is shown in the figures, Holtz and Kovacs (1981). Instead, the failure envelope was curved, leaving the angle of internal friction and cohesion values open to interpretation.

From the plot of log (E_{50}) vs. log(σ_h / ρ) for the conventional triaxial compression test, the following equation was derived:

$$E_{50} = 2.0 \left(\sigma_h / \rho \right)^{0.6}$$

This relationship was derived from the results of only three tests and cannot be considered accurate without further verification in the form of additional tests at higher confining stresses.

CHAPTER 7 SUMMARY

7.1 Effect of Low Vacuum on Density and Stress-Strain-Strength Behavior

The purpose of this study, in the broadest sense, was to provide a basis for future work to investigate the stress-strain-strength behavior of lunar soil. In both the pilot study and the tests conducted in the vacuum triaxial chamber; vacuum level had no major effect on the ultimate density or the stress-strain-strength behavior of the lunar soil simulant. However, the vacuum levels and confining stresses used in this research were sufficient to prove the design of and refine the operating procedures for the vacuum triaxial chamber.

Vey and Nelson (1965), had described significant effects of vacuum on porosity of loosely deposited lunar soil simulant. To some extent, the results of density / cyclic load tests of this investigation were similar to these observations. Other researchers found increases in interparticle friction and compressive strength of lunar soil simulants in vacuum (Chapter 2). The major difference between this study and previous work was the vacuum levels at which the tests were conducted. Investigators who found

vacuum to have an effect on strength behavior operated experiments in the ultra-high vacuum range of 10^{-9} torr to 10^{-14} torr. The vacuum levels employed in this study were in the low vacuum range (10^{-1} torr to 10^{-4} torr), Roth (1976).

To adequately model lunar soil would require vacuum triaxial tests at a variety of confining stresses, some of large magnitude. This investigation considered only low confining stresses, the largest of which represented a depth of approximately 1.5 m (5 ft) of lunar soil in lunar gravity.

7.2 Suggested Procedural and Equipment Modifications

Before more meaningful work to investigate the stress-strain-strength behavior of lunar soil can be attempted, some limitations imposed by equipment design or operating characteristics need to be removed. Improvements can be made in three specific areas: higher vacuum levels can be employed, greater confining stresses placed on samples in the vacuum triaxial chamber, and the erratic loading occurring at the initiation of the vacuum triaxial tests can be eliminated.

The vacuum pumping system and the chamber used for this investigation were capable of achieving and sustaining vacuum in the order of 10^{-7} torr. However, the limiting

component was the vacuum gage which measured the pressure in the chamber. The Pirani gage used for this research had a useful range from atmospheric pressure to 10^{-4} torr. Obtaining a gage that is more compatible with the vacuum pumping system would allow tests to be run at higher vacuum levels.

Greater confining stresses, resulting in sample strengths which would require the MTS controller to operate in the high load/low resolution mode, could be used in the vacuum triaxial tests. Automatic or pre-programmed control of the rate of strain during the tests would eliminate the need for manual control of the sample loading rate which is impossible at the high load/low resolution setting. The hardware to provide this pre-programmed control is currently available in the Constitutive Modeling Laboratory (CML) at the Department of Civil Engineering and Engineering Mechanics. The software needed for this particular function is in the final stages of development at the CML.

Disproportionate loading at the onset of the vacuum triaxial tests resulted in unconventional states of stress occurring in the samples. The sudden rise in confining stress from zero to 15 psi as the air inlet of the chamber was opened was the cause of these non-hydrostatic stress states. A vacuum gage and vacuum gate valve installed at

the air inlet would provide the control necessary to gradually increase the confining stress from zero. A corresponding gradual increase in vertical stress would reduce disproportionate loading and maintain semi-hydrostatic stresses on the sample.

These three modifications are desirable prior to continuing research using this vacuum triaxial chamber. With these modifications in place, subsequent investigations can employ a broader range of variables and expand on the basic research presented in this report.

REFERENCES

Bowles, J.E., Foundation Analysis and Design: Fourth Edition, McGraw-Hill, Inc., New York, NY, 1988

Carrier,D.W. III; Bromwell,L.G.; Martin,R.T., 1973, "Behavior of Returned Lunar Soil in Vacuum", Journal of Soil Mechanics and Foundations Div.,ASCE, Nov. '73, SM11, pp. 979-996

Carrier, W.D. and Mitchell, J.K., "Geotechnical Engineering on the Moon", Proc. One Day Seminar on Planetary Excavation, Bernold, L.E., Ed., University of Maryland; College Park, MD, 1989

Costes, N.C.; Carrier, W.D.; Mitchell, J.K.; Scott, R.F., "Apollo 11: Soil Mechanics Results", J. Soil Mech. and Found. Div., ASCE, SM-6, Nov., 1970

Fuenkajorn,K., Daemen,J.J.K., "Experimental Assessment of Borehole Wall Drilling Damage in Basaltic Rocks", University of Arizona, Dept. of Mining and Geologic Engineering, Tucson, AZ, NUREG 1 CR-4641, 1986, pg. 32.

Holtz, R.D. and Kovacs, W.D., An Introduction to Geotechnical Engineering; Printice-Hall, Inc., Englewood Cliffs, NJ, 1981

Johnson,S.W., Pyrz,A.P., Lee,D.G., and Thompson,J.E., "Simulating the Effects of Gravitational Field and Atmosphere on Behavior of Granular Media", J. Spacecraft, vol.7, No.11, November, 1970.

Land, P., "Lunar Base Design", Lunar Bases and Space Activities of the 21st Century, Mendell, W.W., Ed., 1985

Melzer, K.J., "Methods for Investigating Strength Characteristics of a Lunar Soil Simulant", Geotechnique, 24, No. 1, 1974, pp 13-20.

Nowatzki,E.A.,"The Effects of Thermal and Ultrahigh Vacuum Environment on the Strength of Precompressed Granular Materials", Communication presented at the Conference on Lunar Geophysics, October 18-21,1971, Lunar Science Institute, Houston,TX

Scott, R.F., "Mechanical Properties of Lunar Surface Material", Powder Technology, 3, Elsevier Sequoia S.A., Lausanne, Netherlands, 1969

Taylor, S.R., Lunar Science: A Post Apollo View, Pergamon Press, Inc., Elmsford, NY, 1975

Roth, A., Vacuum Technology, American Elsevier Pub. Co., New York, NY, 1976

Vey,E. and Nelson,J.D. "Engineering Properties of Simulated Lunar Soils", Jnl of Soil Mech. & Found. Div. ASCE, Jan. 1965, SM-1, 25-52